

Sequential Monte Carlo approximations of Wasserstein–Fisher–Rao gradient flows

Francesca Romana Crucinio*¹ and Sahani Pathiraja†²

¹ESOMAS, University of Turin, Italy & Collegio Carlo Alberto, Turin, Italy

²School of Mathematics & Statistics, UNSW Sydney, Australia

Abstract

We consider the problem of sampling from a probability distribution π . It is well known that this can be written as an optimisation problem over the space of probability distribution in which we aim to minimise the Kullback–Leibler divergence from π . We consider several partial differential equations (PDEs) whose solution is a minimiser of the Kullback–Leibler divergence from π and connect them to well-known Monte Carlo algorithms. We focus in particular on PDEs obtained by considering the Wasserstein–Fisher–Rao geometry over the space of probabilities and show that these lead to a natural implementation using importance sampling and sequential Monte Carlo. We propose a novel algorithm to approximate the Wasserstein–Fisher–Rao flow of the Kullback–Leibler divergence which empirically outperforms the current state-of-the-art. We study tempered versions of these PDEs obtained by replacing the target distribution with a geometric mixture of initial and target distribution and show that these do not lead to a convergence speed up.

Contents

1	Introduction	2
2	Gradient flow PDEs for sampling	4
2.1	Convergence properties	5
2.2	Tempered PDEs for sampling	6
3	An importance sampling approach to approximate the WFR PDE	8
3.1	Tempered WFR PDE	10
3.2	Convergence properties	11
4	Sampling Algorithms and Gradient Flow PDEs	11
4.1	Approximations to Pure Fisher–Rao Dynamics	12
4.2	Approximations to Wasserstein–Fisher–Rao Dynamics	12
4.3	Sequential Monte Carlo as Approximation of WFR Flows	13
4.3.1	Unit Time FR flow	13
4.3.2	WFR flow	15
4.3.3	Tempered WFR flow	15
4.3.4	Convergence Properties	16

*francescaromana.crucinio@unito.it F.R.C. gratefully acknowledges the “de Castro” Statistics Initiative at the *Collegio Carlo Alberto* and the *Fondazione Franca e Diego de Castro*.

†s.pathiraja@unsw.edu.au S.P. gratefully acknowledges funding from UNSW Faculty of Science Research Grant and the Eva Mayr Stihl Foundation.

5	Numerical Experiments	17
5.1	Birth Death Langevin and sequential Monte Carlo Wasserstein Fisher Rao	17
5.2	Tempered and Standard PDEs	18
5.3	Tempered SMC-WFR and Tempering SMC	19
6	Conclusion	19
A	Supplementary Lemmata	25
B	Convergence Results	26
B.1	Convergence of Continuous Time Schemes	26
B.1.1	Wasserstein Fisher Rao Flow	26
B.1.2	Tempered Wasserstein PDE	26
B.1.3	Tempered Fisher Rao PDE	27
B.1.4	Tempered Wasserstein Fisher Rao PDE	28
B.1.5	Gradient flow structure of tempered PDEs	29
B.2	Convergence of Discrete Time Schemes	29
B.2.1	Proof of Proposition 3.1	29
B.2.2	Proof of Proposition 3.2	30
B.2.3	Auxiliary results for the proof of Proposition 3.2	31
B.3	Convergence of Sequential Monte Carlo Approximations	34
B.3.1	Auxiliary results for the proof of Proposition 4.1	34
C	Analytic solutions: Multivariate Gaussian case	37
D	Algorithms and Additional Experimental Results	39
D.1	Birth Death Langevin Algorithms	39
D.2	Additional results for Gaussian Mixture	39

1 Introduction

Sampling from a target probability distribution whose density is known up to a normalisation constant is a fundamental task in computational statistics and machine learning. A natural way to formulate this task is optimisation of a functional measuring the dissimilarity to the target probability distribution, typically the Kullback–Leibler (KL) divergence.

Following this point of view, one can derive many popular sampling frameworks including variational inference [BKM17], algorithms based on the Langevin dynamics [RS02, DMM19] and on kernelised Langevin dynamics [LW16]. When the space over which the optimisation is carried out is the Wasserstein space, i.e. probability distributions with bounded second moments equipped with the Wasserstein-2 distance [AGS08], the resulting gradient descent scheme is referred to as Wasserstein (W) gradient flow. It is well-known that the W gradient flow of the KL can be implemented by a Langevin diffusion [JKO98, Wib18] and easily discretised in time, resulting for instance in the Unadjusted Langevin algorithm (ULA; [RT96, DMM19]) and in the Metropolis-adjusted Langevin Algorithm (MALA; [RS02]) when a Metropolis–Hastings accept reject step is added after each discretisation step. Convergence of the W gradient flow and of the Unadjusted Langevin algorithm is guaranteed when the target distribution is sufficiently smooth and verifies a log-Sobolev assumption [VW19]. Alternative time discretisations of the KL Wasserstein gradient flow [SKL20, MMW+21] or its gradient flow with respect to similar optimal transport geometries have been considered in the literature to propose alternative algorithms [LW16, GIHLS20], but their convergence also depends strongly on the log-concavity of the target.

A second class of gradient flows which has gained popularity in recent years is that of Fisher–Rao (FR) gradient flows, i.e. gradient descent w.r.t. the Fisher–Rao or Hellinger–Kakutani distance. Contrary to the Wasserstein metric, which leads to a diffusive behaviour, the Fisher–Rao metric leads to birth-death dynamics in which mass is created or removed. FR gradient flows perform natural gradient descent (see, e.g., [Nüs24, Appendix D] and [FA95, HS98, Har09a]).

Exponential convergence of the FR gradient flow for KL does not require a log-Sobolev assumption and can be established under a bounded second moment assumption and mild regularity of the ratio between target and initial distribution [CHH⁺23b, Theorem 4.1], and therefore holds for a wider class of targets. The FR gradient flow for KL is intimately tied to tempering or annealing due to its unit time rescaling [DEP23, CHH⁺24] and can also be connected to a mirror descent optimisation scheme for KL [CCK24]. While superior in terms of theoretical behaviour, the FR gradient flow does not naturally lead to stable algorithms, in fact, as noted in [CHH⁺24], pure FR dynamics cannot change the support of the distribution, so additional steps need to be added to explore the space. These steps can change the dynamics and can become problematic in high dimensions.

One option to address this shortcoming is offered by kernel methods [Nüs24, MM24, WN24] which naturally introduce a diffusive part into the (unit time) FR dynamics. A second option, and the main focus of this paper, is to combine the W and the FR gradient flows by making use of the Wasserstein–Fisher–Rao metric [GM17] leading to the Wasserstein–Fisher–Rao (WFR) gradient flow. The WFR flow combines the diffusive behaviour of the W gradient flow with the FR flow and enjoys more favourable convergence properties, combining the rate of convergence of the W flow with that of the FR flow [DEP23, LLN19]; its numerical approximation can considerably speed up the convergence of gradient based methods for multimodal targets [LLN19, LSW23] and has been successfully employed to learn Gaussian mixtures [YWR24]. Despite its favourable convergence properties, the WFR flow of the KL has remained relatively understudied compared to the W and the FR flow. This is likely due to the difficulty of obtaining stable numerical approximations for the WFR flow. To the best of our knowledge, the only numerical approximations of the WFR flow for the reverse KL are given by the birth-death Langevin algorithms developed in [LLN19, LSW23].

In this paper we review the main gradient flows used for sampling with particular focus on the Wasserstein–Fisher–Rao flow due to its superior convergence properties (Section 2). We propose an algorithm to approximate the WFR flow of the KL divergence which combines the diffusive behaviour of Langevin based algorithms with importance sampling (Section 3) and empirically show its superior performance w.r.t. the birth-death Langevin dynamics of [LLN19, LSW23].

We further explore the connections between the FR gradient flow, importance sampling and sequential Monte Carlo samplers (SMC; [dMDJ06]) and identify in the latter a general framework to approximate different FR flows. While connections between sequential Bayesian inference and FR flows have been explored in the discrete time and discrete space setting [DM97, Sha09, Har09b, Aky17, CGTS22] and more recently in continuous time and continuous space [PW24]; our focus here is on the sampling problem, in which no underlying sequential structure is present. We also propose a new method whereby importance sampling is used for the FR part.

To further explore the connection with SMC we consider also *tempered* versions of the W, FR and WFR PDEs obtained by considering a time varying target $\pi_t \propto \pi^{\lambda_t} \mu_0^{1-\lambda_t}$ for $\lambda_t : \mathbb{R}_+ \rightarrow [0, 1]$. We explore their gradient flow structure and show that these tempered PDEs do not improve the continuous time convergence rate of their non-tempered counterparts as shown in [CKSV25] for the W flow.

To summarise, the main contributions of this work are

- We show that in the continuous time setting, tempering the target π does not improve convergence speed for the Wasserstein and the Fisher–Rao flow (Proposition 2.1 and 2.2).
- We propose stable algorithms to approximate the WFR flow which combine the diffusive behaviour of Langevin samplers and importance sampling (Algorithm 1) and establish their convergence properties (Proposition 3.1 and 3.2). We empirically show that they outperform the current approximations of the WFR flow. We then show that these algorithms are a particular instance of sequential Monte Carlo samplers.
- We provide an optimisation point of view on sequential Monte Carlo samplers, showing that they provide numerical approximations of many FR type gradient flows of the Kullback–Leibler divergence. We thus establish a parallel result to that of [JKO98, Wib18] which shows that algorithms based on the Langevin diffusion can be seen as numerical approximations of the Wasserstein gradient flow.

Notation We define some notation that will be used throughout the manuscript. We endow \mathbb{R}^d with the Borel σ -field $\mathcal{B}(\mathbb{R}^d)$ with respect to the Euclidean norm $\|\cdot\|$ when d is clear from context. We denote by

$C^1(\mathbb{R}^d)$ the set of continuously differentiable functions, for all $f \in C^1(\mathbb{R}^d)$ we denote the gradient by ∇f . Furthermore, if f is twice differentiable we denote by $\nabla^2 f$ its Hessian and by Δf its Laplacian. We denote by $\mathcal{P}_{ac}(\mathbb{R}^d)$ the set of probability measures over $\mathcal{B}(\mathbb{R}^d)$ which admit a density w.r.t. the Lebesgue measure. The Kullback–Leibler divergence is defined as follows: for $\nu, \mu \in \mathcal{P}_{ac}(\mathbb{R}^d)$, $D_{\text{KL}}(\nu|\mu) = \int \log(\nu(x)/\mu(x))\nu(x)dx$. Throughout this manuscript we denote the target by π and assume $\pi \propto \exp(-V)$ for some $V \in C^1(\mathbb{R}^d)$. The initial distribution of each flow is denoted by μ_0 and μ_t is the density at time t , with unnormalised density ρ_t .

2 Gradient flow PDEs for sampling

Let us denote the target distribution over \mathbb{R}^d by π and assume that it admits a density w.r.t. the Lebesgue measure also denoted by π , then a natural way to recover π is to consider the optimisation problem

$$\min_{\mu \in \mathcal{P}(\mathbb{R}^d)} D_{\text{KL}}(\mu|\pi),$$

which can be solved by following the direction of steepest descent of $D_{\text{KL}}(\cdot|\pi)$, given by the gradient flow partial differential equation (PDE)

$$\partial_t \mu_t = -\text{grad}_{\mathfrak{m}} D_{\text{KL}}(\mu_t|\pi),$$

where $\text{grad}_{\mathfrak{m}} D_{\text{KL}}(\mu|\pi)$ denotes the gradient of $D_{\text{KL}}(\cdot|\pi)$ w.r.t. metric \mathfrak{m} [AGS08, CCH⁺24]. Depending on the choice of metric \mathfrak{m} , the gradient $\text{grad}_{\mathfrak{m}} \mathcal{F}(\mu)$ takes different shapes; we primarily focus on Wasserstein (W), Fisher–Rao (FR) and Wasserstein–Fisher–Rao (WFR) flows of the Kullback–Leibler divergence in infinite time.

The gradient flow of $D_{\text{KL}}(\mu|\pi)$ w.r.t. the geometry induced by the Wasserstein distance is given by

$$\partial_t \mu_t(x) = \nabla \cdot \left(\mu_t(x) \nabla \log \left(\frac{\mu_t(x)}{\pi(x)} \right) \right) \quad t \in [0, \infty) \quad (2.1)$$

and corresponds to the Fokker-Planck equation of a Langevin diffusion targeting π [JKO98]. Convergence of the W gradient flow has been widely studied [DMM19, VW19] and is guaranteed whenever π satisfies a log-Sobolev inequality (e.g., [CEL⁺24]).

The Fisher–Rao (FR) gradient flow of $D_{\text{KL}}(\mu|\pi)$ is obtained by considering the Fisher–Rao (also known as Hellinger) metric [LLN19]

$$\partial_t \mu_t(x) = \mu_t(x) \left(\log \left(\frac{\pi(x)}{\mu_t(x)} \right) - \mathbb{E}_{\mu_t} \left[\log \left(\frac{\pi}{\mu_t} \right) \right] \right) \quad t \in [0, \infty), \quad (2.2)$$

and is closely tied to mirror descent [CCK24, DEP23] and birth-death [LLN19, LSW23] dynamics.

Combining the two geometries one obtains the Wasserstein–Fisher–Rao (WFR) gradient flow [LLN19, Theorem 3.1]

$$\partial_t \mu_t(x) = \mu_t(x) \left(\log \left(\frac{\pi(x)}{\mu_t(x)} \right) - \mathbb{E}_{\mu_t} \left[\log \left(\frac{\pi}{\mu_t} \right) \right] \right) + \nabla \cdot \left(\mu_t(x) \nabla \log \left(\frac{\mu_t(x)}{\pi(x)} \right) \right) \quad t \in [0, \infty), \quad (2.3)$$

where the addition of the two components is justified because each is π -invariant. As we will see later, from a sampling point of view the W flow diffuses the samples “horizontally” and promotes exploration of the space while the FR flows “vertically” weights the samples according to their closeness to the target π . Intuitively, the combination of these two strategies will improve on each one of them.

Fisher–Rao gradient flows are easily rescaled to the unit time interval as shown in [DEP23] and in Lemma A.2 in a slightly more condensed form. The unit time FR PDE takes the form

$$\partial_t \mu_t(x) = \mu_t(x) \left(\log \left(\frac{\pi(x)}{\mu_0(x)} \right) - \mathbb{E}_{\mu_t} \left[\log \left(\frac{\pi}{\mu_0} \right) \right] \right) \quad t \in [0, 1] \quad (2.4)$$

and is the basis of recently developed kernel-based algorithms [MM24, Nüs24]. This PDE is not a gradient flow for D_{KL} but minimises the negative log-likelihood

$$\mathcal{F}^1(\mu) = \int \log \left(\frac{\mu_0(x)}{\pi(x)} \right) \mu(x) dx \quad (2.5)$$

w.r.t. the Fisher–Rao distance [PW24, Lemma 2.1]. This functional is not lower bounded and thus the corresponding minimisation problem is not well-posed. However, at time $t = 1$ the solution of the unit-time FR flow coincides with π .

The unit time FR flow is intimately tied to geometric interpolations or annealing [CCK24, DEP23] which are at the basis of sequential Monte Carlo (SMC; [dMDJ06]), annealed importance sampling (AIS; [Nea01]), parallel tempering (PT; [Gey91]) and the homotopy method [DH08]. This can be seen assuming that the unnormalised sequence of densities is constructed via a geometric interpolation $\rho_t = \pi^t \mu_0^{1-t} = e^{t \log \pi} e^{(1-t) \log \mu_0}$ for $t \in [0, 1]$. Differentiating ρ_t with respect to time and applying Lemma A.1 with $f(x) = \log \pi(x) - \log \mu_0(x)$ yields the unit time FR PDE (2.4).

2.1 Convergence properties

We briefly review the convergence properties of the WFR flow to showcase its superior theoretical properties compared to the FR and the W flow. The infinite-time FR flow (2.2) minimises $D_{\text{KL}}(\mu|\pi)$ w.r.t. the Fisher–Rao distance (e.g., [PW24, Lemma 2.1]); a similar results holds for the W flow (2.1) w.r.t. the Wasserstein-2 distance under a log-Sobolev assumption on the target π (e.g., [CEL⁺24]):

$$D_{\text{KL}}(\mu|\pi) \leq \frac{C_{\text{LSI}}}{2} \int \mu \|\nabla \log \frac{\mu}{\pi}\|^2 \quad (2.6)$$

where C_{LSI} denotes the log-Sobolev constant of π . The convergence of (2.2) to π has been investigated in [LLN19, LSW23, DEP23, CHH⁺23b]. To the best of our knowledge, the most general convergence result is given in [CHH⁺23b, Theorem 4.1] and requires that μ_0, π have bounded second moments $\int \|x\|^2 \mu_0(x) dx \leq B$, $\int \|x\|^2 \pi(x) dx \leq B$ and

$$e^{-M(1+\|x\|^2)} \leq \frac{\mu_0(x)}{\pi(x)} \leq e^{M(1+\|x\|^2)} \quad (2.7)$$

for some $M > 0$. Under these assumptions, we have

$$D_{\text{KL}}(\mu_t|\pi) \leq M(2 + B + B e^{M(1+B)e^{-t}}) e^{-t}. \quad (2.8)$$

We point out that this rate is not sharp in general, as can be seen by setting $t = 0$. To obtain the rate of decay of D_{KL} for the WFR flow we consider the time derivative of $D_{\text{KL}}(\mu_t|\pi)$ along the WFR flow

$$\frac{d}{dt} D_{\text{KL}}(\mu_t|\pi) = \int \log \frac{\mu_t}{\pi} \partial_t \mu_t = - \int \mu_t \|\nabla \log \frac{\mu_t}{\pi}\|^2 - \int \mu_t \left(\log \frac{\mu_t}{\pi} \right)^2 + D_{\text{KL}}(\mu_t|\pi)^2. \quad (2.9)$$

As observed in [GM17, page 13], the first term corresponds to the negative gradient of D_{KL} w.r.t. the Wasserstein-2 metric, while the remaining terms give the negative gradient of D_{KL} w.r.t. the Fisher–Rao geometry, implying that the dissipation for the WFR metric is the sum of the W and the FR dissipation. As a consequence, the convergence rate of WFR gradient flow (2.3) can be upper bounded by

$$D_{\text{KL}}(\mu_t|\pi) \leq \min \{ D_{\text{KL}}(\mu_t^{\text{FR}}|\pi), D_{\text{KL}}(\mu_t^{\text{W}}|\pi) \},$$

where $\mu_t^{\text{FR}}, \mu_t^{\text{W}}$ denote the solutions of the FR and W flow PDEs respectively. Using (2.8) and known results for the convergence of the W flow (e.g., [CEL⁺24]) we find that

$$D_{\text{KL}}(\mu_t|\pi) \leq \min \left\{ M(2 + B + B e^{M(1+B)e^{-t}}) e^{-t}, D_{\text{KL}}(\mu_0|\pi) e^{-2C_{\text{LSI}}^{-1}t} \right\}, \quad (2.10)$$

where C_{LSI} denotes the log-Sobolev constant of π .

Under stronger assumptions on the ratio μ_0/π and a warm-start condition detailed in Appendix B.1, [LLN19] obtain a tighter convergence rate for all $t \geq t_0 := \log(M/\delta^3)$ and $\delta > 0$:

$$D_{\text{KL}}(\mu_t|\pi) \leq e^{-(2C_{\text{LSI}}^{-1} + (2-3\delta))(t-t_0)} D_{\text{KL}}(\mu_0|\pi). \quad (2.11)$$

This result obtained in [LLN19, Appendix B] confirms the rate conjectured by [DEP23] based on their numerical experiments and shows that combining the W flow and the FR flow leads to a considerable speed up.

We point out that neither (2.10) nor (2.11) provide a sharp rate of decay for $D_{\text{KL}}(\mu_t|\pi)$. In fact, (2.10) shows that the rate of WFR is never worse than that of W or FR, looking at (2.9) however it is evident that the rate of decay of the WFR flow should be considerably higher than that of the two singular flows. Similarly, (2.11) shows that the decay in the case of the WFR flow is faster than that of the W flow but the rate depends on an arbitrary constant δ which makes (2.11) harder to interpret.

2.2 Tempered PDEs for sampling

We consider a second class of PDEs in which the target π is replaced by a sequence of moving targets $(\pi_t)_{t \geq 0}$. These samplers have become popular in the literature with the hope that the introduction of moving targets will improve the convergence of the sampler [NVPB24, AVE24, CKSV25, GTC25].

We focus here on the sequence $(\pi_t)_{t \geq 0}$ defined by the geometric tempering iteration $\pi_t \propto \pi^{\lambda_t} \mu_0^{1-\lambda_t}$ where the tempering schedule $\lambda_t : \mathbb{R}_+ \rightarrow [0, 1]$, λ_t is non-decreasing in t and weakly differentiable. This corresponds to the solution of the unit time FR flow (2.4) and has been popularised in the sampling literature through its use in sequential Monte Carlo (SMC; [dMDJ06]), annealed importance sampling (AIS; [Nea01]), parallel tempering (PT; [Gey91]) and the homotopy method [DH08].

Recently, [CKSV25] proposed tempered unadjusted Langevin algorithms as an approximation of the FR flow in unit time when μ_0, π are continuously differentiable. The corresponding PDE is given by

$$\partial_t \mu_t(x) = \nabla \cdot \left(\mu_t(x) \nabla \log \left(\frac{\mu_t(x)}{\pi_t(x)} \right) \right) \quad t \in [0, \infty). \quad (2.12)$$

This PDE is not a gradient flow of $D_{\text{KL}}(\mu|\pi)$ and thus decay of $D_{\text{KL}}(\mu|\pi)$ along the flow needs to be checked directly.

Tempered unadjusted Langevin algorithms (Tempered ULA; [CKSV25]) provide an approximation of the tempered PDE (2.12) by using an Euler discretisation of the associated SDE

$$dX_t = \nabla \log \pi_t(X_t) dt + \sqrt{2} dB_t. \quad (2.13)$$

[CKSV25, Corollary 5 and 6] show that if V_π is strongly log-convex with constant c_π and similarly for V_{μ_0} , and $c_\pi \geq c_{\mu_0}/2$ then $\lambda_t \equiv 1$ is optimal and the tempered W PDE does not improve on the standard W flow (2.1).

Given the tempering sequence π_t , one can also define the tempered FR PDE

$$\partial_t \mu_t = \mu_t(x) \left(\log \left(\frac{\pi_t(x)}{\mu_t(x)} \right) - \mathbb{E}_{\mu_t} \left[\log \left(\frac{\pi_t}{\mu_t} \right) \right] \right). \quad (2.14)$$

Similarly to (2.12), the PDE (2.14) is not a gradient flow of $D_{\text{KL}}(\mu|\pi)$. As we show later, (2.12) reduces $D_{\text{KL}}(\mu|\pi)$ at a rate which is always worse than that of the standard FR PDE (2.2).

Given the tempered W and tempered FR PDE one can naturally define a tempered WFR PDE

$$\partial_t \mu_t = \nabla \cdot \left(\mu_t(x) \nabla \log \left(\frac{\mu_t(x)}{\pi_t(x)} \right) \right) + \mu_t(x) \left(\log \left(\frac{\pi_t(x)}{\mu_t(x)} \right) - \mathbb{E}_{\mu_t} \left[\log \left(\frac{\pi_t}{\mu_t} \right) \right] \right). \quad (2.15)$$

As we show in the following sections, a particular discretisation of this PDE coincides with the commonly used tempering approaches in sequential Monte Carlo samplers [dMDJ06]. Appendix B.1.5 establishes that the tempered PDEs can be seen as gradient flows of a functional \mathcal{F} defined on the product space $\mathcal{P}(\mathbb{R}^d) \times [0, 1]$.

We now analyse the decay of the Kullback–Leibler along the different tempered PDEs and compare it with their standard non-tempered counterparts. In order to obtain our results and allow comparison between

the tempered PDEs (2.12) and (2.14) and their standard counterpart (2.1) and (2.2) we make the following assumptions on π, μ_0 . These assumptions are strong but somewhat classical in the study of convergence of Langevin based samplers (e.g., [DMM19, CKSV25]).

Assumption 1. We assume that $\pi \propto e^{-V_\pi}$ with $V_\pi \in C^1(\mathbb{R}^d)$ and that for all $x, x' \in \mathbb{R}^d$

(a) there exists $L_\pi > 0$ such that $\|\nabla V_\pi(x) - \nabla V_\pi(x')\| \leq L_\pi \|x - x'\|$;

(b) there exists $c_\pi > 0$ such that $\langle x - x', \nabla V_\pi(x) - \nabla V_\pi(x') \rangle \geq c_\pi \|x - x'\|^2$.

Assumption 2. We assume that $\mu_0 \propto e^{-V_{\mu_0}}$ with $V_{\mu_0} \in C^1(\mathbb{R}^d)$ and that for all $x, x' \in \mathbb{R}^d$

(a) there exists $L_{\mu_0} > 0$ such that $\|\nabla V_{\mu_0}(x) - \nabla V_{\mu_0}(x')\| \leq L_0 \|x - x'\|$;

(b) there exists $c_{\mu_0} > 0$ such that $\langle x - x', \nabla V_{\mu_0}(x) - \nabla V_{\mu_0}(x') \rangle \geq c_{\mu_0} \|x - x'\|^2$.

Assumption 1-(b) implies that π satisfies (2.6) with $C_{LSI} = c_\pi^{-1}$. Assumption 2 combined with Assumption 1 implies that $\nabla V_{\pi_t} := (1 - \lambda_t)\nabla V_{\mu_0} + \lambda_t\nabla V_\pi$ is Lipschitz continuous with Lipschitz constant $L_{\pi_t} = (1 - \lambda_t)L_{\mu_0} + \lambda_t L_\pi$ and strongly convex with constant $c_{\pi_t} \geq (1 - \lambda_t)c_{\mu_0} + \lambda_t c_\pi$.

Under Assumption 1 and 2 we can obtain a result similar to [CKSV25, Theorem 1] (see Appendix B.1 for a proof). Our result carries the same message as [CKSV25, Theorem 1] but allows for an easier comparison between tempered and standard PDEs.

Proposition 2.1 (Tempered W). *Under Assumption 1 and 2, the tempered W PDE (2.12) reduces the Kullback–Leibler divergence at rate*

$$D_{\text{KL}}(\mu_t|\pi) \leq e^{-2tC_{LSI}^{-1}}D_{\text{KL}}(\mu_0|\pi) + A \int_0^t e^{-2(t-s)C_{LSI}^{-1}}(1 - \lambda_s)ds, \quad (2.16)$$

where $C_{LSI} = c_\pi^{-1}$, $A < \infty$ is a constant which only depends on the convexity and Lipschitz properties of V_π, V_{μ_0} . The convergence rate of the standard W PDE (2.1) is recovered for $\lambda_s \equiv 1$.

The first term corresponds to the rate of the classical W PDE (2.1), to which a bias term is added due to the fact that π_t approaches π only as $t \rightarrow \infty$.

Under the same assumptions required to obtain the convergence results for the standard FR PDE (2.8), we can obtain convergence of the tempered FR PDE (2.14) (see Appendix B.1 for a proof).

Proposition 2.2 (Tempered FR). *Assume that $\int \|x\|^2 \mu_0(x)dx \leq B$, $\int \|x\|^2 \pi(x)dx \leq B$ and (2.7). The tempered FR PDE (2.14) reduces the Kullback–Leibler divergence at rate*

$$D_{\text{KL}}(\mu_t|\pi) \leq M(1 - \int_0^t e^{s-t}\lambda_s ds) \left[2 + B + B \exp\left(M(1+B)(1 - \int_0^t e^{s-t}\lambda_s ds)\right) \right], \quad (2.17)$$

from which we recover (2.8) in the case $\lambda_s \equiv 1$.

Since $1 - \int_0^t e^{s-t}\lambda_s ds - e^{-t} = \int_0^t e^{s-t}(1 - \lambda_s)ds \geq 0$, we conclude that the tempered FR PDE does not improve on the convergence rate of the standard FR PDE.

Exploiting the fact that the time derivative of D_{KL} along the tempered WFR PDE factorises into two terms as in the case of the standard WFR flow, we can show that, if μ_t follows the tempered WFR flow (2.15),

$$D_{\text{KL}}(\mu_t|\pi) \leq \min \{D_{\text{KL}}(\mu_t^{\text{T-W}}|\pi), D_{\text{KL}}(\mu_t^{\text{T-FR}}|\pi)\}; \quad (2.18)$$

where an upper bound to $D_{\text{KL}}(\mu_t^{\text{T-W}}|\pi)$ is given in (2.16) and one for $D_{\text{KL}}(\mu_t^{\text{T-FR}}|\pi)$ in (2.17).

Our results as well as those in [CKSV25] suggest that the tempered dynamics do not improve on the gradient flow ones discussed in the previous section. However, our convergence results only obtain upper bounds for the decay of D_{KL} which are not necessarily tight. To confirm that the tempered PDEs do not improve over the standard ones, we consider the case of 1D Gaussian distributions, for which the W, FR, WFR, and their tempered versions can be solved analytically.

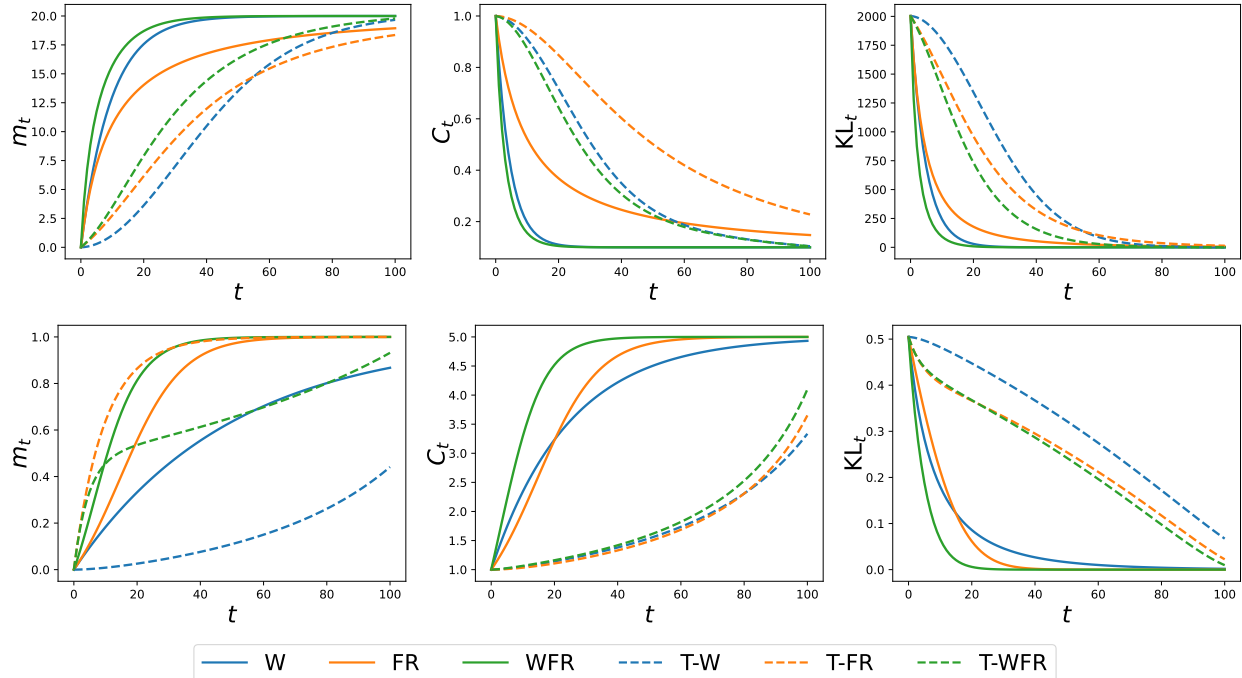


Figure 2.1: Evolution of mean, variance and KL along different PDE flows in the 1D Gaussian case with $\mu_0(x) = \mathcal{N}(x; 0, 1)$ and $\pi(x) = \mathcal{N}(x; 20, 0.1)$ (first row), $\pi(x) = \mathcal{N}(x; 1, 5)$ (second row).

Figure 2.1 shows the evolution of mean, covariance and Kullback–Leibler divergence along different PDE flows in the case of 1D Gaussians. For the tempered PDEs we use the linear schedule $\lambda_s = s/t$. The initial distribution is a standard Gaussian and we consider two different targets: for target 1 (first row) we set $m_\pi = 20, \sigma_\pi^2 = 0.1$. In this case the W flow is clearly faster than the FR one and the WFR flow behaves more like the W flow (Figure 2.1 top row). For the second target (second row) we have $m_\pi = 1, \sigma_\pi^2 = 5$; the FR flow is faster than the W flow for all sufficiently large t , and the WFR flow more closely follows the FR flow. Figure 2.1 confirms our theoretical results: (a) the tempered PDEs result in a slower convergence to the target than the corresponding standard flows and (b) combining the W flow with the FR flow improves on both the W flow and the FR flow.

3 An importance sampling approach to approximate the WFR PDE

The infinite time Wasserstein–Fisher–Rao PDE takes the form

$$\partial_t \mu_t = f_W(\mu_t) + f_{FR}(\mu_t)$$

where $f_W(\mu) := \nabla \cdot (\mu \nabla \log \frac{\mu}{\pi})$ and $f_{FR}(\mu) := \mu (\log \frac{\pi}{\mu} - \int \log \frac{\pi}{\mu} d\mu)$ correspond to the Wasserstein and Fisher–Rao operators respectively, and takes the form of a reaction-diffusion equation.

To obtain a time discretisation of the WFR PDE we consider the solution operator of the W flow and the FR flow separately. Assume that for certain discrete time $n - 1$ the solution of the WFR PDE is given by μ_{n-1} , then applying the W flow for a time step γ leads to

$$\begin{aligned} \mu_{n-1/2}(x) &:= \mathcal{N}(0, 2\gamma \cdot \text{Id}) * [(\text{Id} + \gamma \nabla \log \pi) \# \mu_{n-1}](x) \\ &\propto \int \exp\left(-\frac{1}{2\gamma} \|x - y - \gamma \nabla \log \pi(y)\|^2\right) \mu_{n-1}(y) dy, \end{aligned} \tag{3.1}$$

see, e.g. [Wib18]. The FR flow is not a linear operator, therefore to obtain an explicit expression for its action on $\mu_{n-1/2}$ we consider the solution of the infinite time unnormalised FR PDE,

$$\partial_t \rho_t = \rho_t \log \frac{\pi}{\rho_t} \quad (3.2)$$

over time period t , where the above is obtained by applying Lemma A.1 to (2.2). We can evaluate (3.2) directly using the substitution $\nu_t := \log \frac{\rho_t}{\pi}$ which transforms (3.2) into a linear PDE [CHH⁺23b, Eq. (B.1)],

$$\partial_t \nu_t = \frac{\partial_t \rho_t}{\rho_t} = \log \frac{\pi}{\rho_t} = -\nu_t$$

which has explicit solution $\nu_t = \nu_0 e^{-t} = e^{-t} \log \frac{\rho_0}{\pi}$. Transforming back yields

$$e^{-t} \log \frac{\rho_0}{\pi} = \log \frac{\rho_t}{\pi} \implies \rho_t = \pi^{1-e^{-t}} \cdot \rho_0^{e^{-t}}.$$

Therefore, we immediately obtain that the FR flow with time step γ applied to $\mu_{n-1/2}$ gives

$$\mu_n(x) := \pi(x)^{1-e^{-\gamma}} \mu_{n-1/2}(x)^{e^{-\gamma}} = \left(\frac{\pi(x)}{\mu_{n-1/2}(x)} \right)^{1-e^{-\gamma}} \mu_{n-1/2}(x). \quad (3.3)$$

The evolution in (3.1) and (3.3) describes one step of the WFR in discrete time; we now show that both the W and the FR flow can be naturally implemented via sampling based ideas.

We consider an initial state for the WFR PDE given by the empirical measure $\mu_0^N = N^{-1} \sum_{i=1}^N \delta_{X_0^i}$ where $X_0^i \sim \mu_0$ for $i = 1, \dots, N$. Given $\mu_{n-1}^N = N^{-1} \sum_{i=1}^N \delta_{X_{n-1}^i}$, an empirical measure approximating μ_{n-1} , we can approximate the W flow in (3.1) exploiting the well-known connections between the W flow and Langevin dynamics [JKO98], a discretisation of (3.1) over timestep γ is given by the following unadjusted Langevin (ULA) scheme

$$X_n = X_{n-1} + \gamma \nabla \log \pi(X_{n-1}) + \sqrt{2\gamma} \xi_n, \quad (3.4)$$

where $\xi_n \sim \mathcal{N}(0, \text{Id})$. The empirical measure $\mu_{n-1/2}^N := N^{-1} \sum_{i=1}^N \delta_{X_n^i}$ provides an approximation to $\mu_{n-1/2}$.

The solution of the FR flow (3.3) corresponds to one step of mirror descent applied to the Kullback–Leibler divergence (see [CCK24]), starting from $\mu_{n-1/2}$ we obtain μ_n as

$$\mu_n \propto \mu_{n-1/2}^{1-\delta} \pi^\delta, \quad (3.5)$$

with $\delta = 1 - e^{-\gamma}$. Given $\mu_{n-1/2}^N$, μ_n can be approximated by importance sampling with unnormalised weights given by $w_n(x) = \left(\frac{\pi(x)}{\mu_{n-1/2}^N(x)} \right)^{1-e^{-\gamma}}$. Observing that when approximating the WFR flow via the FR step is applied after the W step, we can compute the weights as

$$\begin{aligned} w_n(x) &= \left(\frac{\pi(x)}{\mu_{n-1/2}^N(x)} \right)^{1-e^{-\gamma}} = \left(\frac{\pi(x)}{\mathcal{N}(0, 2\gamma \cdot \text{Id}) * [(\text{Id} + \gamma \nabla \log \pi) \# \mu_{n-1}^N](x)} \right)^{1-e^{-\gamma}} \\ &= \left(\frac{\pi(x)}{N^{-1} \sum_{i=1}^N \mathcal{N}(x; X_{n-1}^i + \gamma \nabla \log \pi(X_{n-1}^i), 2\gamma \cdot \text{Id})} \right)^{1-e^{-\gamma}}, \end{aligned} \quad (3.6)$$

where we used the definition of pushforward measure and convolution integral to obtain the last expression. This gives the following importance sampling approximation to μ_n : $\mu_n^N := \sum_{i=1}^N W_n^i \delta_{X_n^i}$ where $W_n^i \propto w_n(X_n^i)$.

Alternating between one step of W flow approximated via (3.4) and one step of FR flow approximated via importance sampling with weights (3.6) we obtain an approximation of WFR PDE through sampling-based procedures (Algorithm 1). To avoid the weight degeneracy normally introduced by repeated importance sampling steps, after each FR step we add a resampling step [JSDT11]. We will show in Section 4.3 that this approximation of the WFR PDE is an instance of a well known class of Monte Carlo algorithms: sequential Monte Carlo samplers.

Algorithm 1 SMC-WFR.

- 1: *Inputs*: learning rate γ , initial proposal μ_0 .
- 2: *Initialize*: sample $\tilde{X}_0^i \sim \mu_0$ and set $W_0^i = 1/N$ for $i = 1, \dots, N$.
- 3: **for** $n = 1, \dots, T$ **do**
- 4: **if** $n > 1$ **then**
- 5: *Resample*: draw $\{\tilde{X}_{n-1}^i\}_{i=1}^N$ independently from $\{X_{n-1}^i, W_{n-1}^i\}_{i=1}^N$ and set $W_n^i = 1/N$ for $i = 1, \dots, N$.
- 6: **end if**
- 7: *W flow*: update $X_n^i = \bar{X}_{n-1}^i + \sqrt{2\gamma}\xi_{n-1/2}^i$, where $\bar{X}_{n-1}^i = \tilde{X}_{n-1}^i + \gamma\nabla \log \pi(\tilde{X}_{n-1}^i)$, $\xi_{n-1/2}^i \sim \mathcal{N}(0, \text{Id})$ for $i = 1, \dots, N$.
- 8: *FR flow*: compute and normalize the weights $W_n^i \propto w_n(X_n^i)$ for $i = 1, \dots, N$, where

$$w_n(x) = \left(\frac{\pi(x)}{\frac{1}{N} \sum_{i=1}^N \mathcal{N}(x; \bar{X}_{n-1}^i, 2\gamma \cdot \text{Id})} \right)^{1-e^{-\gamma}}$$

- 9: **end for**
 - 10: *Output*: $\{X_n^i, W_n^i\}_{i=1}^N$
-

3.1 Tempered WFR PDE

We briefly describe how to obtain a numerical approximation similar to Algorithm 1 for the tempered WFR PDE (2.15). We denote by $\pi_n \propto \pi^{\lambda_{t_n}} \mu_0^{1-\lambda_{t_n}}$ obtained by considering a time discretisation $0 = \lambda_{t_0} \leq \lambda_{t_1} \leq \dots \leq \lambda_{t_n} \leq \lambda_{t_{n+1}} \leq \dots$ of $\lambda_t : \mathbb{R}_+ \rightarrow [0, 1]$ with $t_{n+1} - t_n = \gamma$. Given μ_{n-1} , applying the tempered W flow over time step γ gives

$$\mu_{n-1/2}(x) \propto \int \exp\left(-\frac{1}{2\gamma}\|x - y - \gamma\nabla \log \pi_n(y)\|^2\right) \mu_{n-1}(y) dy,$$

which can be implemented using the tempered ULA scheme of [CKSV25]:

$$X_n = X_{n-1} + \gamma\nabla \log \pi_n(X_{n-1}) + \sqrt{2\gamma}\xi_n, \quad (3.7)$$

where $\xi_n \sim \mathcal{N}(0, \text{Id})$.

The tempered Fisher–Rao flow is also a non linear operator. Following an approach similar to that in (3.2) detailed in (B.4) we find that the action of the tempered FR flow over time step γ is given by

$$\mu_n(x) = \mu_{n-1/2}(x) e^{-\gamma + \int_0^\gamma e^{s-\gamma}(1-\lambda_s) ds} \pi(x) \int_0^\gamma e^{s-\gamma} \lambda_s ds = \left(\frac{\pi(x)}{\mu_{n-1/2}(x)} \right)^{\int_0^\gamma e^{s-\gamma} \lambda_s ds} \mu_{n-1/2}(x), \quad (3.8)$$

where we used $e^{-t} + \int_0^t e^{s-t}(1-\lambda_s) ds = 1 - \int_0^t e^{s-t} \lambda_s ds$, which corresponds to mirror descent (3.5) with $\delta = \int_0^\gamma e^{s-\gamma} \lambda_s ds$.

Thus, if a particle approximation μ_{n-1}^N of μ_{n-1} is available, we can approximate the tempered WFR PDE by applying one step of tempered ULA (3.7) to each particle and then importance sampling with unnormalised weights

$$w_n(x) = \left(\frac{\pi(x)}{N^{-1} \sum_{i=1}^N \mathcal{N}(x; X_{n-1}^i + \gamma\nabla \log \pi_n(X_{n-1}^i), 2\gamma \cdot \text{Id})} \right)^{\int_0^\gamma e^{s-\gamma} \lambda_s ds}. \quad (3.9)$$

Alternating between one step of tempered W flow approximated via (3.7) and one step of tempered FR flow approximated via importance sampling with weights (3.9) we obtain an approximation of tempered WFR PDE through sampling-based procedures. A resampling step to avoid the weight degeneracy normally introduced by repeated importance sampling steps can also be added. We will show in Section 4.3 that this approximation of the tempered WFR PDE is an instance of a well known class of Monte Carlo algorithms: sequential Monte Carlo samplers.

3.2 Convergence properties

Combining the fact that the mirror descent iterates (3.5) reduce the Kullback–Leibler divergence as established in [AFKL22, CCK24] and standard results on the convergence of the unadjusted Langevin algorithm [VW19], we can establish that the discrete scheme given by (3.4)–(3.5) converges exponentially fast provided that the stepsize γ is chosen wisely (see Appendix B.2 for a proof).

Proposition 3.1. *Assume that π satisfies the log-Sobolev inequality (2.6) and Assumption 1-(a), if $\gamma \leq C_{LSI}^{-1}/(4L_\pi^2)$ the approximation of the WFR flow given by (3.4)–(3.5) with $\delta = 1 - e^{-\gamma}$ satisfies*

$$D_{\text{KL}}(\mu_n|\pi) \leq e^{-n\gamma/C_{LSI}} D_{\text{KL}}(\mu_0|\pi) + 8\gamma d L_\pi^2 C_{LSI}^{-1}.$$

The first term of the bound in Proposition 3.1 shows that (3.4)–(3.5) reduce the Kullback–Leibler divergence exponentially fast up to an error due to the time discretisation in (3.4). Comparing Proposition 3.1 with [VW19, Theorem 1] we find that, also in discrete time, the rate of WFR is never worse than that of pure W.

As in the continuous time case, obtaining a sharp rate of convergence for the WFR flow is challenging. Our proof techniques uses results from the mirror descent literature which only show that the FR part reduces the Kullback–Leibler divergence but do not quantify the reduction in terms of rates, thus the rate in Proposition 3.1 coincides with that of the discrete time W flow in [VW19, Theorem 1] and is not sharp in general.

A result equivalent to Proposition 3.1 can also be established for the tempered scheme under a strong convexity assumption on both target and initial distribution (see Appendix B.2 for a proof).

Proposition 3.2. *Under Assumption 1 and 2, if $\gamma_n \leq \min(1, c_{\pi_n}/4L_{\pi_n}^2, (c_{\pi_n} - 1/(2\epsilon))/L_{\pi_n}^2)$ with $\epsilon > 1/(2c_{\pi_n})$ for all $n \geq 1$ the approximation of the Tempered WFR flow given by (3.7)–(3.5) with $\delta_n = \int_0^{\gamma_n} e^{s-\gamma_n} \lambda_s ds$ satisfies*

$$\begin{aligned} D_{\text{KL}}(\mu_n|\pi) &\leq D_{\text{KL}}(\mu_0|\pi) e^{-\sum_{k=1}^n \gamma_k c_{\pi_k}} + 2d \sum_{k=1}^n \gamma_k L_{\pi_k} e^{-\sum_{i=1}^k \gamma_i c_{\pi_i}} \\ &\quad + 2A \sum_{k=0}^{n-1} \gamma_k (1 - \lambda_k) e^{-\sum_{i=1}^k \gamma_i c_{\pi_i}} + \sum_{k=0}^{n-1} \gamma_k (1 - \lambda_k) B_k e^{-\sum_{i=1}^k \gamma_i c_{\pi_i}}, \end{aligned}$$

where $A < \infty$ is a constant which only depends on the convexity and Lipschitz properties of V_π, V_{μ_0} and B_k is a constant which grows exponentially with k .

The first line of the bound in Proposition 3.2 shows that (3.7)–(3.5) reduce the Kullback–Leibler divergence exponentially fast up to an error due to the time discretisation in (3.7). The additional terms are due to the bias in the tempered dynamics, which only target π asymptotically and disappear when $\lambda_n \equiv 1$. As for the case of the standard WFR flow this result is not sharp in general, as the decay rate of D_{KL} along the tempered FR flow is not quantified precisely.

4 Sampling Algorithms and Gradient Flow PDEs

We now discuss some popular and recent algorithms which approximate the gradient flows of $D_{\text{KL}}(\mu|\pi)$. We focus on those approximating the FR flow and the WFR flow as connections between W flows and their numerical approximations have been widely studied [JKO98, Wib18, DMM19]. We briefly review algorithms which are known and then focus on approaches which already exist in the literature but whose connection with gradient flows is less well known.

There is a reach literature of embedding the PDEs describing W, FR and WFR flows in reproducible kernel Hilbert spaces (RKHS) which led to a number of “kernelised” algorithms (e.g. [LW16, MM24, Nüs24]). We do not consider those in this paper and leave their analysis for future work.

Method	Geometry	Requires gradients
Birth Death Langevin [LSW23, LLN19]	WFR	✓
Mirror Descent [KP22, DHDS16]	Infinite Time FR	✗
SMC with RWB	Unit Time FR	✗
SMC with ULA	WFR	✓
SMC with Tempered ULA	Tempered WFR	✓
Tempered ULA [CKSV25]	Tempered W	✓

Table 1: Popular and novel algorithms approximating gradient flows. Our proposed algorithms combine sequential Monte Carlo (SMC) with different proposal kernels.

4.1 Approximations to Pure Fisher–Rao Dynamics

As discussed in Section 3, the solution operator of the infinite time FR flow corresponds to the mirror descent iterates (3.5). [DHDS16, KP22, BDPP24] propose algorithms based on importance sampling which approximate the mirror descent iterates; however, due to the lack of transport dynamics of the mirror descent iterates (3.5) additional approximation steps are needed: [DHDS16] considers a smoothed version of (3.5) obtained by convolution of μ_n with a smoothing kernel K at each step; [KP22, BDPP24] use a “safe density” q_0 and replace the approximation of μ_n , denoted q_n , with the mixture $r q_0 + (1 - r) q_n$ for $r \in [0, 1]$ at each iteration. This guarantees stability of the algorithm but incurs an additional approximation of (3.5). In fact, as noted in [CHH⁺24], pure FR dynamics cannot change the support of the distribution, so additional steps need to be added to explore the space. These steps can change the dynamics and can become problematic in high dimensions.

Approximations of the unit time FR PDE (2.4) can be obtained considering the tempering iterates

$$\mu_{n+1} \propto \mu_0^{1-\lambda_{n+1}} \pi^{\lambda_{n+1}}. \quad (4.1)$$

These sequence of distributions is often used in sequential Monte Carlo (SMC; [dMDJ06]), annealed importance sampling (AIS; [Nea01]), parallel tempering (PT; [Gey91]) and the homotopy method [DH08] to bridge between an easy-to-sample-from initial distribution μ_0 to the target π . The tempering iterates (4.1) can be obtained from the unit time FR PDE via a forward time discretisation. Setting $\lambda_n = 1 - \prod_{k=1}^n (1 - \delta_k)$ it is easy to show that (4.1) is a time rescaling of (3.5) as shown in [CCK24], which gives an equivalent result to Lemma A.2 in discrete time.

4.2 Approximations to Wasserstein–Fisher–Rao Dynamics

Birth Death Langevin (BDL) algorithms were introduced in [LSW23, LLN19] as an approximation of the WFR flow. They consider the PDE (2.3) and replace μ_t with an empirical measure leading to an interacting particle system whose evolution is then discretised in time. The W step is performed via the unadjusted Langevin algorithm (ULA) with target π , as in (3.4); while the FR step is performed via a birth-death step with exact rate

$$\Lambda(x, \mu_t) := \log \left(\frac{\mu_t}{\pi} \right) - \mathbb{E}_{\mu_t} \left[\log \left(\frac{\mu_t}{\pi} \right) \right]. \quad (4.2)$$

When μ_t is replaced by an empirical measure μ_t^N , the rate $\Lambda(x, \mu_t)$ cannot be computed analytically and [LLN19] resort to kernel density estimation (KDE) and replace μ_t^N with $K_\varepsilon * \mu_t^N$, where K_ε is a kernel with bandwidth ε . Convergence of the resulting continuous-time interacting particle system is guaranteed by [LLN19, Proposition 5.1].

Contrary to our approach, the BDL dynamics are obtained by first applying a space discretisation (corresponding to the empirical measure μ_t^N) and then a time discretisation. The W step described by the Fokker–Planck PDE (2.1) is resolved using a time discretisation of the corresponding Langevin SDE and the FR flow (2.2) is resolved through its connections with birth-death processes. Different approximations of the rate (4.2) lead to slightly different BDL algorithms [LSW23, PHHV23].

4.3 Sequential Monte Carlo as Approximation of WFR Flows

We introduce in this section a class of algorithms known as sequential Monte Carlo samplers [dMDJ06] and highlight how different algorithmic choices within this class lead to approximations of the PDE flows described in Section 2, including Algorithm 1.

Sequential Monte Carlo (SMC) samplers [dMDJ06] provide a particle approximation of the sequence of distributions $(\hat{\eta}_n)_{n \geq 0}$ using clouds of N weighted particles $\{X_n^i, W_n^i\}_{i=1}^N$. To build an SMC sampler approximating the sequence $(\hat{\eta}_n)_{n \geq 0}$ one needs a family of Markov kernels $(M_n)_{n \geq 1}$ used to propagate forward the particles, a sequence of backward kernels $(L_{n-1})_{n \geq 1}$ and a resampling scheme.

A resampling scheme is a selection mechanism which given a set of weighted samples $\{X^i, W^i\}_{i=1}^N$ outputs a sequence of equally weighted samples $\{\tilde{X}^i, 1/N\}_{i=1}^N$ in which $\tilde{X}^i = X^j$ for some j for all $i = 1, \dots, N$. For a review of commonly used resampling schemes see [GCW19].

At iteration n the weighted particle set $\{X_{n-1}^i, W_{n-1}^i\}_{i=1}^N$ approximating $\hat{\eta}_{n-1}$ is resampled to obtain the equally weighted particle set $\{\tilde{X}_{n-1}^i, 1/N\}_{i=1}^N$ and the kernel M_n is applied to propose new particle locations $X_n^i \sim M_n(\tilde{X}_{n-1}^i, \cdot)$. At this stage the particle set approximates $\hat{\eta}_{n-1}$, to obtain an approximation of $\hat{\eta}_n$ an importance sampling step is applied with weights proportional to

$$w_n(x_{n-1}, x_n) = \frac{\hat{\eta}_n(x_n) L_{n-1}(x_n, x_{n-1})}{\hat{\eta}_{n-1}(x_{n-1}) M_n(x_{n-1}, x_n)}. \quad (4.3)$$

The weight functions (4.3) simplify to $w_n(x_n) = \hat{\eta}_n(x_n)/\hat{\eta}_{n-1}(x_n)$ if M_n is a $\hat{\eta}_{n-1}$ -invariant Markov kernel and L_n the corresponding backward kernel. Due to the renormalisation of the weights we do not need the normalising constants of $\hat{\eta}_n, \hat{\eta}_{n-1}$.

The resulting procedure is summarised in Algorithm 2 whose output is a set of weighted samples which approximate $\hat{\eta}_n$. We refer the reader to [CP20] for a comprehensive introduction to SMC. Annealed importance sampling can be obtained from Algorithm 2 by omitting the resampling step; however, since it has been empirically [JSDT11] and theoretically [SBCCD24] shown that the addition of the resampling step improves the accuracy of the algorithm we do not further consider AIS.

Algorithm 2 SMC samplers [dMDJ06].

- 1: *Inputs:* sequences of distributions $(\hat{\eta}_n)_{n \geq 0}$, Markov kernels $(M_n)_{n \geq 1}$, backward kernels $(L_{n-1})_{n \geq 1}$.
 - 2: *Initialize:* set $\lambda_0 = 0$, sample $\tilde{X}_0^i \sim \hat{\eta}_0$ and set $W_0^i = 1/N$ for $i = 1, \dots, N$.
 - 3: **for** $n = 1, \dots, T$ **do**
 - 4: **if** $n > 1$ **then**
 - 5: *Resample:* draw $\{\tilde{X}_{n-1}^i\}_{i=1}^N$ independently from $\{X_{n-1}^i, W_{n-1}^i\}_{i=1}^N$ and set $W_n^i = 1/N$ for $i = 1, \dots, N$.
 - 6: **end if**
 - 7: *Propose:* draw $X_n^i \sim M_n(\tilde{X}_{n-1}^i, \cdot)$ for $i = 1, \dots, N$.
 - 8: *Reweight:* compute and normalize the weights $W_n^i \propto w_n(\tilde{X}_{n-1}^i, X_n^i)$ in (4.3) for $i = 1, \dots, N$.
 - 9: **end for**
 - 10: *Output:* $\{X_n^i, W_n^i\}_{i=1}^N$
-

There is a vast literature on choosing the sequence $(\hat{\eta}_n)_{n \geq 0}$, proposal kernels and the corresponding backward kernel L_n . We now discuss how different choices lead to numerical approximation of the PDEs described above.

4.3.1 Unit Time FR flow

Consider $\hat{\eta}_n$ to be the n -th tempering iterate (4.1) and as Markov kernel M_n a simple random walk Metropolis (RWM) kernel targeting $\hat{\eta}_{n-1}$. Since this choice of M_n leaves $\hat{\eta}_{n-1}$ invariant, the weights simplify to $w_n(x_n) = \hat{\eta}_n(x_n)/\hat{\eta}_{n-1}(x_n)$. This SMC algorithm approximates the FR flow in unit time (2.4) as observed by [CCK24]. Figure 4.1 first row compares the approximation provided by Algorithm 2 and the evolution of the unit time FR flow for a 1D Gaussian distribution $\pi(x) = \mathcal{N}(x; 20, 0.1)$.

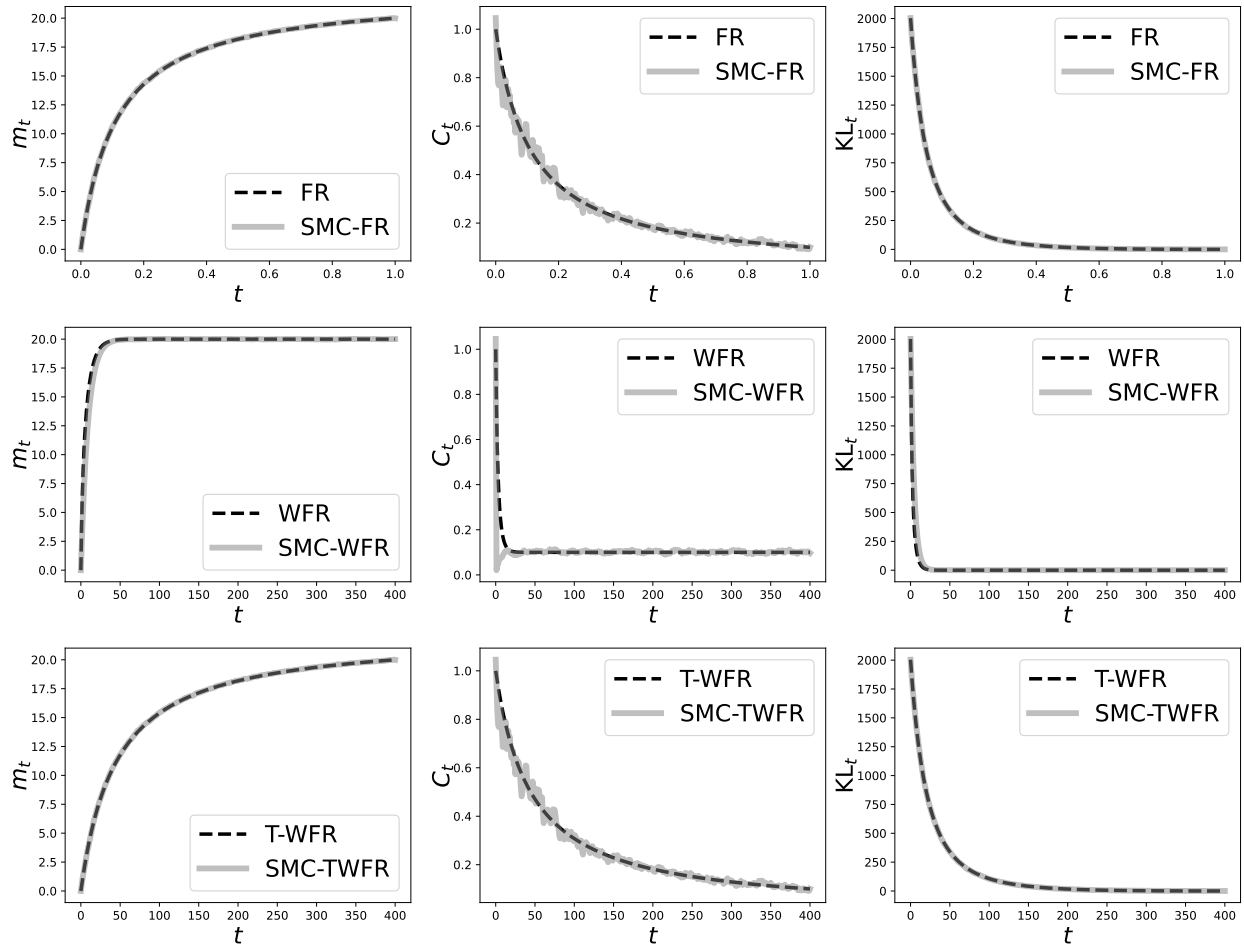


Figure 4.1: Comparison of evolution of mean, variance and KL of the exact PDE flows and approximations provided by Algorithm 2 with target distribution the 1D Gaussian $\pi(x) = \mathcal{N}(x; 20, 0.1)$ and initial distribution $\mu_0(x) = \mathcal{N}(x; 0, 1)$. Top row: Unit time Fisher-Rao; middle row: Wasserstein-Fisher-Rao, bottom row: tempered Wasserstein-Fisher-Rao.

As previously observed for other algorithms approximating the pure FR dynamics, it is necessary to introduce some transport dynamics to obtain a numerical approximation of the FR flow. The introduction of the Metropolis step guarantees that the random walk kernel has the appropriate invariant measure. This was not necessary in Algorithm 1 since both the FR and the W part have the same invariant distribution.

4.3.2 WFR flow

Consider Algorithm 2 with sequence of distributions $(\hat{\eta}_n)_{n \geq 0}$ as (3.5) with $\delta = 1 - e^{-\gamma}$ and M_n given by one step of an unadjusted Langevin algorithm targeting π

$$M_n(x_{n-1}, x_n) = x_{n-1} + \gamma \nabla \log \pi(x_{n-1}) + \sqrt{2\gamma} \xi_n,$$

where $\xi_n \sim \mathcal{N}(0, \text{Id})$, $\gamma > 0$. The optimal backward kernel L_{n-1} given in [dMDJ06, Proposition 1] is intractable in most cases; a pragmatic choice is given by

$$L_{n-1}(x_n, x_{n-1}) = \frac{\hat{\eta}_{n-1}(x_{n-1}) M_n(x_{n-1}, x_n)}{\int \hat{\eta}_{n-1}(z) M_n(z, x_n) dz} \quad (4.4)$$

which leads to the weights

$$\begin{aligned} w_n^{\text{WFR}}(x_n) &= \frac{\hat{\eta}_n(x_n)}{\int \hat{\eta}_{n-1}(x_{n-1}) \mathcal{N}(x_n; x_{n-1} + \gamma \nabla \log \pi(x_{n-1}), 2\gamma \cdot \text{Id}) dx_{n-1}} \\ &= \frac{\mu_n(x_n)}{\int \mathcal{N}(x_n; x_{n-1} + \gamma \nabla \log \pi(x_{n-1}), 2\gamma \cdot \text{Id}) \mu_{n-1}(x_{n-1}) dx_{n-1}}. \end{aligned} \quad (4.5)$$

For small γ , we can approximate the weights above with

$$\begin{aligned} w_n^{\text{WFR}}(x_n) &= \frac{\mu_{n-1}^{e^{-\gamma}}(x_n) \pi^{1-e^{-\gamma}}(x_n)}{\int \mathcal{N}(x_n; x_{n-1} + \gamma \nabla \log \pi(x_{n-1}), 2\gamma \cdot \text{Id}) \mu_{n-1}(x_{n-1}) dx_{n-1}} \\ &\approx \left(\frac{\pi(x_n)}{\int \mathcal{N}(x_n; x_{n-1} + \gamma \nabla \log \pi(x_{n-1}), 2\gamma \cdot \text{Id}) \mu_{n-1}(x_{n-1}) dx_{n-1}} \right)^{1-e^{-\gamma}} \\ &\approx \left(\frac{\pi(x_n)}{N^{-1} \sum_{i=1}^N \mathcal{N}(x_n; X_{n-1}^i + \gamma \nabla \log \pi(X_{n-1}^i), 2\gamma \cdot \text{Id})} \right)^{1-e^{-\gamma}} := w_n^{\text{WFR}, N}(x_n). \end{aligned}$$

which coincides with (3.6). Different approximations are possible, we choose this one for its similarity with Algorithm 1.

Similarly to the approximations of mirror descent [DHDS16, KP22, BDPP24] and of birth death Langevin algorithms [LLN19, LSW23], the cost of computing the approximate weights is linear in N . However, in our case the mixture approximating the denominator is not obtained from a kernel density estimator introduced purely for numerical purposes, but can be justified from the point of view of the W flow. We directly compare this approximation of the WFR flow with the provided by the Birth Death Langevin dynamics in Section 5.

It is now easy to see that the SMC sampler in Algorithm 2 with sequence of distributions $(\hat{\eta}_n)_{n \geq 0}$ as (3.5), M_n as the unadjusted Langevin kernel and L_{n-1} the approximation of the optimal kernel discussed in [dMDJ06, Section 3.3.2.1] coincides with Algorithm 1 and provides an approximation of the WFR flow. This connection allows us to exploit the wide literature on convergence of SMC samplers to obtain a convergence results for Algorithm 1 (see Section 4.3.4) and provides a natural way to estimate the normalising constant of π [dMDJ06, Section 3.2]. Figure 4.1 second row compares the approximation provided by Algorithm 2 and the evolution of the WFR flow for a 1D Gaussian distribution $\pi(x) = \mathcal{N}(x; 20, 0.1)$.

4.3.3 Tempered WFR flow

Take now Algorithm 2 with sequence of distributions $(\hat{\eta}_n)_{n \geq 0}$ as (3.5) with $\delta = \int_0^\gamma e^{s-\gamma} \lambda_s ds$ and M_n given by a discretisation of the tempered Langevin SDE (2.13)

$$M_n(x_{n-1}, x_n) = x_{n-1} + \gamma \nabla \log \pi_n(x_{n-1}) + \sqrt{2\gamma} \xi_n, \quad (4.6)$$

where $\gamma > 0$ is a stepsize, $\xi_n \sim \mathcal{N}(0, \text{Id})$ and $\pi_n \propto \pi^{\lambda_n} \mu_0^{1-\lambda_n}$ for $0 = \lambda_0 < \lambda_1 < \dots < \lambda_n \dots \leq 1$. Using the approximation to the optimal backward kernel L_{n-1} in (4.4) leads to the weights

$$w_n(x_n) = \frac{\hat{\eta}_n(x_n)}{\int \hat{\eta}_{n-1}(x_{n-1}) \mathcal{N}(x_n; x_{n-1} + \gamma \log \pi_n(x_{n-1}), 2\gamma \cdot \text{Id}) dx_{n-1}}. \quad (4.7)$$

Approximating the weights above as shown in the previous section, we find

$$w_n^{\text{T-WFR}}(x_n) \approx \left(\frac{\pi(x_n)}{N^{-1} \sum_{i=1}^N \mathcal{N}(x_n; X_{n-1}^i + \gamma \nabla \log \pi_n(X_{n-1}^i), 2\gamma \cdot \text{Id})} \right)^{\int_0^\gamma e^{s-\gamma} \lambda_s ds} := w_n^{\text{T-WFR}, N}(x_n).$$

which coincides with (3.9). It is now easy to see that the SMC sampler in Algorithm 2 provides an approximation of the Tempered WFR flow by selecting the sequence of distributions $(\hat{\eta}_n)_{n \geq 0}$ as (3.5), M_n as the unadjusted tempered Langevin kernel and L_{n-1} the approximation of the optimal kernel discussed in [dMDJ06, Section 3.3.2.1]. Figure 4.1 third row compares the approximation provided by Algorithm 2 and the evolution of the tempered WFR flow for a 1D Gaussian distribution $\pi(x) = \mathcal{N}(x; 20, 0.1)$.

Despite using the tempered unadjusted Langevin algorithm as proposal, this SMC approximation of the tempered WFR flow does not coincide with the standard tempering SMC sampler [CP20, Chapter 17]. To draw a connection between the tempered WFR flow and tempering SMC, consider the tempered FR PDE (2.14); instead of using the exact evolution (3.8) consider an explicit time discretisation with stepsize $\delta > 0$

$$\log(\mu_{n+1}) - \log(\mu_n) = -\delta \left(\log \left(\frac{\mu_n}{\pi_{n+1}} \right) - \mathbb{E}_{\mu_n} \left[\log \left(\frac{\mu_n}{\pi_{n+1}} \right) \right] \right).$$

As for the mirror descent iterates (3.5), $\mathbb{E}_{\mu_n} \left[\log \left(\frac{\mu_n}{\pi_{n+1}} \right) \right]$ is just a normalising constant, and we obtain the sequence of distributions

$$\mu_{n+1} \propto \mu_n^{(1-\delta)} \pi_{n+1}^\delta = \mu_n^{(1-\delta)} \pi^{\lambda_{n+1} \delta} \mu_0^{(1-\lambda_{n+1}) \delta} = \pi^{\lambda_{n+1}} \mu_0^{(1-\lambda_{n+1})} \quad (4.8)$$

when $\delta \equiv 1$. Using this sequence of distributions with the tempered unadjusted Langevin proposal (4.6) coincides with the commonly used tempering SMC and results in weights $w_n(x_n) = (\pi(x_n)/\mu_0(x_n))^{\lambda_n - \lambda_{n-1}}$ for sufficiently small γ [DHJW22].

4.3.4 Convergence Properties

Algorithm 2 provides an approximation of the WFR and tempered WFR flow for particular choices of the sequence $(\hat{\eta}_n)_{n \geq 0}$ and of proposal kernel M_n ; however, the weights in (4.5) and (4.7) are intractable due to the presence of the convolution in the denominator and need to be approximated by $w_n^{\text{WFR}, N}$ and $w_n^{\text{T-WFR}, N}$, respectively.

Convergence of the numerical approximations to $\hat{\eta}_n$ provided by Algorithm 2 follow from the rich literature on convergence of SMC methods (e.g. [dM04]) taking into account the additional approximation in the weight function w_n . We provide here a simple result to validate our proposed approach and refer to the vast literature on convergence of SMC methods and their variants for further results (e.g., [dM04]). For simplicity, we focus on the case of measurable bounded test functions $\varphi : \mathbb{R}^d \rightarrow \mathbb{R}$ with $\|\varphi\|_\infty := \sup_{x \in \mathbb{R}^d} |\varphi(x)| < \infty$, a set we denote by $\mathcal{B}_b(\mathbb{R}^d)$. We make the following assumption on the approximated weights w_n^N . While strong, this assumption is standard in the SMC literature and corresponds to the assumption used in [LLN19, Theorem 3.2] to prove the sharper convergence rate in (2.11).

Assumption 3. *The weights w_n^N are positive everywhere, $w_n^N(x_n) > 0$ for every $x_n \in \mathbb{R}^d$, and upper bounded $\|w_n^N\|_\infty := \sup_{x \in \mathbb{R}^d} |w_n^N(x)| < \infty$.*

This assumption and some mild regularity on π (implied by Assumption 1–(b)) allow us to obtain the following weak law of large numbers (WLLN) whose proof is provided in Appendix B.3:

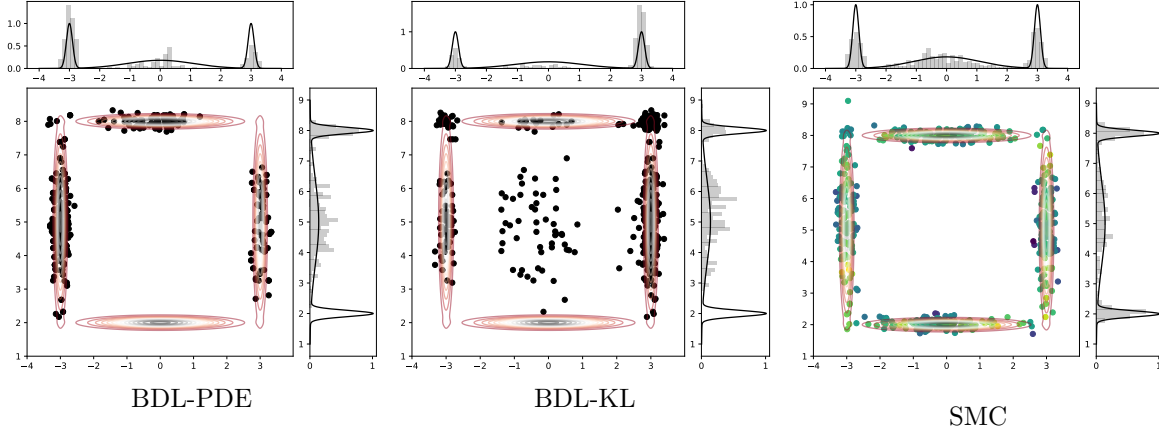


Figure 5.1: Comparison of approximations of the target $\pi(x) = \sum_{i=1}^4 w_i \mathcal{N}(x; m_i, C_i)$ for the birth-death Langevin algorithms and our SMC approximation. For the latter the colour of the particles corresponds to the weight (brighter corresponds to higher weight). We compare both the joint distribution and the marginals.

Proposition 4.1 (Weak law of large numbers). *Under Assumption 3, if π is upper bounded, for all $n \geq 0$ and for every $\varphi \in \mathcal{B}_b(\mathbb{R}^d)$, we have the following convergence in probability*

$$\sum_{i=1}^N W_n^i \varphi(X_n^i) \xrightarrow{P} \int \varphi(x) \hat{\eta}_n(x) dx.$$

5 Numerical Experiments

We now present some numerical experiments to support our results in the previous sections. In particular, we show that SMC-WFR in Algorithm 1 outperforms the birth-death Langevin dynamics as approximation of WFR and compare tempered and standard PDEs. Code to reproduce our experiments is available at <https://github.com/FrancescaCrucinio/SMC-WFR>.

5.1 Birth Death Langevin and sequential Monte Carlo Wasserstein Fisher Rao

We compare the approximation of the WFR flow (2.3) provided by Algorithm 1 with that given by the birth death Langevin (BDL) algorithms of [LSW23, LLN19]. We consider the two dimensional Gaussian mixture of [LLN19], given by $\pi(x) = \sum_{i=1}^4 w_i \mathcal{N}(x; m_i, C_i)$ with

$$w_i = 1/4, i = 1, \dots, 4, m_1 = (0, 8)^T, m_2 = (0, 2)^T, m_3 = (-3, 5)^T, m_4 = (3, 5)^T, \\ \Sigma_1 = \Sigma_2 = \begin{pmatrix} 1.2 & 0 \\ 0 & 0.01 \end{pmatrix}, \Sigma_3 = \Sigma_4 = \begin{pmatrix} 0.01 & 0 \\ 0 & 2 \end{pmatrix}.$$

As shown in [LSW23, LLN19] BDL algorithms significantly outperform ULA on this example due to the presence of four well separated components (see Figure 5.1). We consider two versions of the birth death Langevin algorithm (see Appendix D for details).

The initial distribution μ_0 is a Gaussian with $m_0 = m_1$ and covariance matrix $\Sigma_0 = 0.3 \cdot \text{Id}$. We use $N = 500$, $T = 1000$, $\gamma = 0.05$ and select $h = \gamma$ for the kernel density estimator used within BDL. We compare the results in terms of mean and variance and two distributional metrics: the W_1 distance for each 1D marginal and the maximum mean discrepancy with standard Gaussian kernel (MMD). Both algorithms have $\mathcal{O}(N^2)$ cost due to the computation of the birth death rates and weights, in fact, they also have the same wallclock time when using the same number of iterations and of particles (Table 2).

The results provided by our SMC approximation are considerably better than those obtained by the BDL algorithms. We attribute this improved performance to three factors. First, the approximations of

Method	MSE mean	MSE covariance	W_1	MMD	runtime (s)	MMD < ϵ
BDL-PDE [LLN19]	2.007	4.864	1.320	0.118	13.5	980
BDL-KL [LSW23]	1.892	4.457	1.255	0.112	14.1	971
SMC-WFR	0.005	0.036	0.102	0.003	13.4	281

Table 2: Comparison of the approximation of the WFR flow (2.3) provided by the birth-death Langevin (BDL) algorithms and Algorithm 1. We compare the mean squared error MSE for mean and covariance, the average Wasserstein-1 distance over dimension and the maximum mean discrepancy with Gaussian kernel (MMD). We also report the average runtime and the number of iterations needed to have $\text{MMD} < \epsilon$ for $\epsilon = 0.05$. All results are averaged over 50 replicates.

the birth-death rate (4.2) employed within the BDL algorithms are obtained using kernel density estimation (KDE) while the use of the convolution in (3.6) is motivated by the presence of the W flow and therefore does not add a layer of approximation as does KDE. Secondly, in SMC-WFR the reweighting step corresponds to the exact solution of the FR flow (3.3) in which μ_n is replaced by a particle approximation μ_n^N ; BDL does not use the exact solution but a discretisation of the FR flow obtained through birth-death dynamics. Thirdly, importance (re)sampling seems to be a more algorithmically stable way to approximate the FR flow in the sampling context as it ensures that the number of samples N remains fixed with no additional cost while the BDL dynamics require additional steps to endure that N is kept constant at each time step.

5.2 Tempered and Standard PDEs

Proposition 2.1 shows that the tempered Wasserstein dynamics (T-W) do not improve on the standard Wasserstein gradient flows (W) in the case of strongly log-concave target π . A similar result holds for the WFR flow combining the rates in Proposition 2.1 with those in Proposition 2.2 as shown in (2.18). For bi-modal targets, which satisfy a log-Sobolev assumption but are not log-concave, [CKSV25, Theorem 8] shows that the T-W flow has exponentially slower convergence than the standard W flow.

We empirically show that the same is true for the tempered WFR flow. We consider the same setup of [CKSV25]:

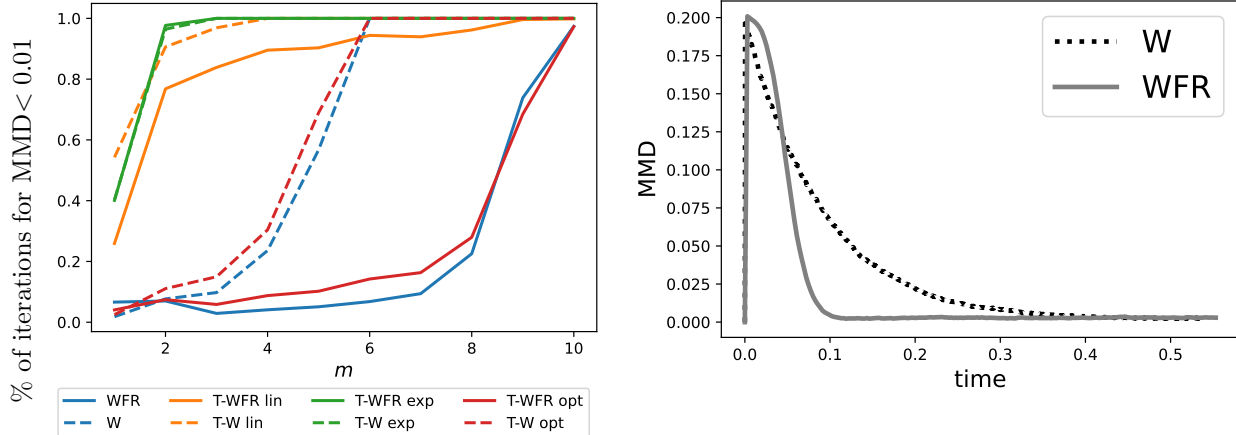
$$\mu_0(x) = \mathcal{N}(x; 0, 1), \quad \pi(x) = \frac{1}{2}\mathcal{N}(x; 0, 1) + \frac{1}{2}\mathcal{N}(x; m, 1). \quad (5.1)$$

This target satisfies a log-Sobolev inequality [Sch19] with $C_{\text{LSI}} = (1 + (e^{m^2} + 1)/2)$.

We numerically approximate the WFR flow using Algorithm 1 and the tempered WFR flow with Algorithm 2 with the proposal and weight functions described in Section 4.3. For the tempered PDEs we consider the linear rate $\lambda_s = s/t$, the exponential rate $\lambda_s = 1 - e^{-\alpha s}$ for $\alpha = 0.01$ and the optimal rate of [CKSV25], $\lambda_s = 1 - 1/(2 + s)$ (which follows from setting $\mu_0(x) = \mathcal{N}(x; 0, 1)$). We check convergence computing the MMD with standard Gaussian kernel.

Figure 5.2(a) shows the number of iteration needed to achieve $\text{MMD} < 0.01$ when $d = 1$. For the W flows we run N parallel chains using the same number of iterations and discretisation steps as for the WFR flows. We see that the tempered dynamics do not perform better than the standard dynamics; the optimal rate performs similarly to the non-tempered dynamics for both W and WFR. WFR converges faster than the W flow for all choices of tempering regardless of the log-Sobolev constant C_{LSI} . The increased convergence speed of WFR comes at a higher computational cost; while ULA and its tempered variants have $\mathcal{O}(N)$ cost, WFR and Tempered WFR require the computation of the weights (4.5) leading to an $\mathcal{O}(N^2)$ cost.

To show that the trade off between computational cost and convergence speed favours WFR over ULA when the two modes are well separated, we plot in Figure 5.2(b) the decay of MMD against wallclock time averaged over 50 replicates for the standard W and WFR flows in the case $m = 6$ for which $C_{\text{LSI}} \approx 2.15561577 \cdot 10^{15}$. WFR is run with $N = 500$ particles for 200 iterations and $\gamma = 0.1$. The results for ULA show the MMD of $N = 500$ independent chains ran for 2000 iterations with $\gamma = 0.1$. Despite the additional cost of computing the weights, WFR converges faster in wallclock time than W; as we show in Appendix D WFR converges to the target π also for larger values of m , for which W fails to reduce the MMD to 0 in the allocate computational budget.



(a) Percent of iterations required to achieve $\text{MMD} < 0.01$ for increasing m . We include standard W & WFR and tempered flows with $\lambda_s = s/t$, $\lambda_s = 1 - e^{-\alpha s}$, $\lambda_s = 1 - 1/(2 + s)$.

(b) MMD decay along the W and WFR flow for $m = 6$.

Figure 5.2: Convergence of approximations to π given by tempered and standard PDE flow with target the Gaussian mixture (5.1). Convergence is measured through the MMD with standard Gaussian kernel and is averaged over 50 replications.

5.3 Tempered SMC-WFR and Tempering SMC

We now compare two approximations of the tempered WFR flow: the usual tempering SMC algorithm (e.g. [CP20]) and the one provided by using the analytic solution of the FR flow. In the first case, we use the sequence $\hat{\eta}_n = \pi^{\lambda_n} \mu_0^{(1-\lambda_n)}$ and tempered ULA (4.6) as proposal kernel in Algorithm 2. In the second case, the proposal kernel is still tempered ULA but the sequence of distributions is given by (3.5), $\hat{\eta}_n = \mu_n \propto \mu_{n-1}^{1-\delta_n} \pi^{\delta_n}$, with $\delta_n = \int_0^{\gamma n} e^{s-\gamma n} \lambda_s ds$.

We empirically compare this two approximations on a 1D Gaussian example with $\mu_0(x) = \mathcal{N}(x; 0, 1)$ and $\pi(x) = \mathcal{N}(x; 20, 0.1)$ using the linear schedule $\lambda_s = s/t$. We take $\gamma \in [0.001, 0.1]$ and investigate how well the two approaches match the exact evolution of D_{KL} along the tempered WFR flow obtained using the moment ODEs in Appendix C. Figure 5.3 shows that for small γ the two approximations are both close to the exact evolution along the tempered WFR PDE but as γ increases tempering SMC deviates from the continuous time evolution by slowing down convergence.

Despite the slower convergence, tempering SMC has some advantages over the approximation of the tempered WFR flow obtained using importance sampling with (3.9) for the tempered FR step: setting $\delta = 1$ in (4.8) results in weights which only involve π, μ_0 and thus can be computed in $\mathcal{O}(1)$ time against the $\mathcal{O}(N)$ time of (3.9). In addition, when using the sequence of distributions $\mu_n \propto \pi^{\lambda_n} \mu_0^{1-\lambda_n}$, one can set $\lambda_T = 1$ for some large T and therefore obtain π in finite time; this is not possible when using the sequence (3.5) with $\delta = \int_0^{\gamma} e^{s-\gamma} \lambda_s ds$ and thus convergence to π only occurs in the infinite time limit.

6 Conclusion

In this paper we study the connection between sampling algorithms and gradient flows in the space of probability measure, with focus on the Fisher–Rao and Wasserstein–Fisher–Rao geometry. We identify a natural parallel between Fisher–Rao dynamics and importance sampling and use this idea to propose several sequential Monte Carlo algorithms which approximate the Wasserstein–Fisher–Rao dynamics. These algorithms have convergence guarantees (Proposition 4.1) and show superior performance to other approximations (Section 5). Connections between the WFR flow and a combination of diffusion and importance weighting

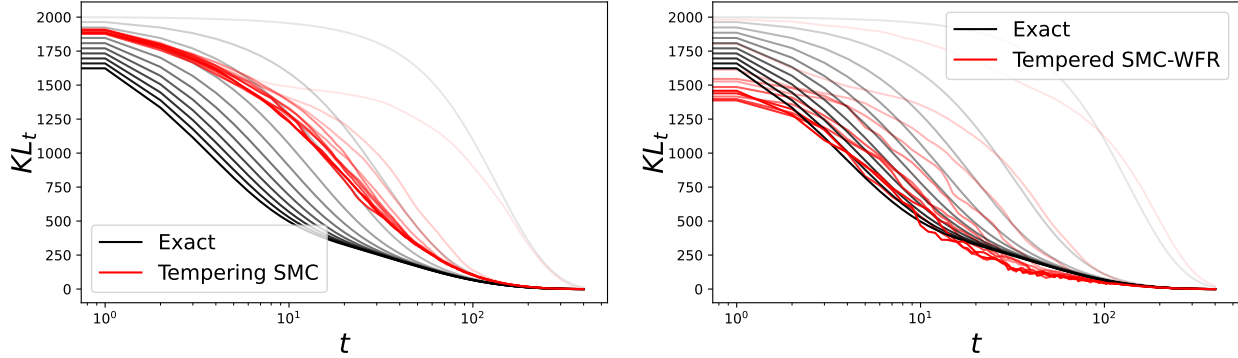


Figure 5.3: Evolution of D_{KL} along the tempered WFR PDE flow with linear schedule and two approximations via SMC. We have $\mu_0(x) = \mathcal{N}(x; 0, 1)$ and $\pi(x) = \mathcal{N}(x; 20, 0.1)$, γ ranges from 0.001 (lighter color) to 0.1 (darker color).

have also been explored in [CNWR25, LCB⁺22, YWR24]. The main difference between our approach and the one of [CNWR25, Section 5.8] is in the order in which the space and time discretisations are performed: [CNWR25, Section 5.8] and [LCB⁺22, Section H] propose to first replace μ with a weighted empirical measure and derive ODEs for the evolution of weights and locations; we first discretise time and connect the solution operators of the W and the FR flow in discrete time to ULA and importance sampling, respectively. This perspective allows us to directly connect the WFR flow with sequential Monte Carlo samplers.

The main drawback of approximating the WFR flow via Algorithm 1 is the $\mathcal{O}(N)$ cost required to compute the weights (4.5); a cheaper alternative could be obtained by selecting a backward kernel L_{n-1} which is not the optimal one (see [dMDJ06] for some examples). This is likely to slow down convergence but would lead to weights which can be computed in $\mathcal{O}(1)$. The best trade off between convergence speed and computational cost will likely be application dependent.

We also consider tempered dynamics and show that, both in continuous and in discrete time this dynamics do not improve the convergence speed of the standard, untempered ones (Proposition 2.1, 2.2, 3.2). Even if our theoretical and empirical results (Section 5) suggest that tempered dynamics are not beneficial for sampling, we point out that the idea of tempering, i.e. to slowly move the initial distribution μ_0 to the target π via a geometric path, coincides with the FR flow, as highlighted in [CCK24, DEP23] (see also the discussion in Section 3). Our results show that adding the FR flow to the W flow dramatically improves convergence by acting in a similar fashion to tempering. Therefore, changing the target in time using $\pi_t \propto \mu_0^{1-\lambda_t} \pi^{\lambda_t}$ only introduces a bias and does not speed up the WFR dynamics.

Acknowledgements The authors would like to thank Deniz Akyildiz, Paula Cordero Encinar, Nikolas Nüsken, Anna Korba, Linfeng Wang for helpful discussions.

F.R.C. is supported by the Gruppo Nazionale per l’Analisi Matematica, la Probabilità e le loro Applicazioni (GNAMPA-INdAM).

References

- [AFKL22] Pierre-Cyril Aubin-Frankowski, Anna Korba, and Flavien Léger. Mirror descent with relative smoothness in measure spaces, with application to Sinkhorn and EM. *Advances in Neural Information Processing Systems*, 35:17263–17275, 2022.
- [AGS08] Luigi Ambrosio, Nicola Gigli, and Giuseppe Savaré. *Gradient flows: in metric spaces and in the space of probability measures*. Springer Science & Business Media, 2008.

- [Aky17] Ömer Deniz Akyildiz. A probabilistic interpretation of replicator-mutator dynamics. *arXiv preprint arXiv:1712.07879*, 2017.
- [AVE24] Michael S Albergo and Eric Vanden-Eijnden. Nets: A non-equilibrium transport sampler. *arXiv preprint arXiv:2410.02711*, 2024.
- [BDPP24] Pascal Bianchi, Bernard Delyon, Victor Priser, and François Portier. Stochastic mirror descent for nonparametric adaptive importance sampling. *arXiv preprint arXiv: 2409.13272*, 2024.
- [BKM17] David M Blei, Alp Kucukelbir, and Jon D McAuliffe. Variational inference: A review for statisticians. *Journal of the American Statistical Association*, 112(518):859–877, 2017.
- [CCH⁺24] José A. Carrillo, Yifan Chen, Daniel Zhengyu Huang, Jiaoyang Huang, and Dongyi Wei. Fisher-Rao Gradient Flow: Geodesic Convexity and Functional Inequalities, 2024. arXiv:2407.15693 [math].
- [CCK24] Nicolas Chopin, Francesca Crucinio, and Anna Korba. A connection between tempering and entropic mirror descent. In Ruslan Salakhutdinov, Zico Kolter, Katherine Heller, Adrian Weller, Nuria Oliver, Jonathan Scarlett, and Felix Berkenkamp, editors, *Proceedings of the 41st International Conference on Machine Learning*, volume 235 of *Proceedings of Machine Learning Research*, pages 8782–8800. PMLR, 21–27 Jul 2024.
- [CDDJ24] Francesca R Crucinio, Valentin De Bortoli, Arnaud Doucet, and Adam M. Johansen. Solving a class of Fredholm integral equations of the first kind via Wasserstein gradient flows. *Stochastic Processes and their Applications*, 173:104374, 2024.
- [CEL⁺24] Sinho Chewi, Murat A Erdogdu, Mufan Li, Ruoqi Shen, and Matthew S Zhang. Analysis of Langevin Monte Carlo from Poincaré to log-Sobolev. *Foundations of Computational Mathematics*, pages 1–51, 2024.
- [CGTS22] Dániel Czégel, Hamza Giaffar, Joshua B. Tenenbaum, and Eörs Szathmáry. Bayes and Darwin: How replicator populations implement Bayesian computations. *BioEssays*, 44(4):1–11, 2022.
- [CHH⁺23a] Yifan Chen, Daniel Zhengyu Huang, Jiaoyang Huang, Sebastian Reich, and Andrew M Stuart. Gradient flows for sampling: mean-field models, Gaussian approximations and affine invariance. *arXiv preprint arXiv:2302.11024*, 2023.
- [CHH⁺23b] Yifan Chen, Daniel Zhengyu Huang, Jiaoyang Huang, Sebastian Reich, and Andrew M Stuart. Sampling via gradient flows in the space of probability measures. *arXiv preprint arXiv:2310.03597*, 2023.
- [CHH⁺24] Yifan Chen, Daniel Zhengyu Huang, Jiaoyang Huang, Sebastian Reich, and Andrew M Stuart. Efficient, multimodal, and derivative-free Bayesian inference with Fisher–Rao gradient flows. *Inverse Problems*, 40(12):125001, 2024.
- [CJ23] Francesca R Crucinio and Adam M Johansen. Properties of marginal sequential Monte Carlo methods. *Statistics & Probability Letters*, 203:109914, 2023.
- [CKPJ25] Rocco Caprio, Juan Kuntz, Samuel Power, and Adam M Johansen. Error bounds for particle gradient descent, and extensions of the log-Sobolev and Talagrand inequalities. *Journal of Machine Learning Research*, 2025+.
- [CKSV25] Omar Chehab, Anna Korba, Austin J Stromme, and Adrien Vacher. Provable convergence and limitations of geometric tempering for langevin dynamics. In *The Thirteenth International Conference on Learning Representations*, 2025.
- [CMR05] Olivier Cappé, Éric Moulines, and Tobyas Rydén. *Inference in hidden Markov models*. Springer, 2005.

- [CNWR25] Sinho Chewi, Jonathan Niles-Weed, and Philippe Rigollet. *Statistical Optimal Transport: École d'Été de Probabilités de Saint-Flour XLIX–2019*, volume 2364. Springer Nature, 2025.
- [CP20] Nicolas Chopin and Omiros Papaspiliopoulos. *An introduction to sequential Monte Carlo*. Springer, 2020.
- [DEP23] Carles Domingo-Enrich and Aram-Alexandre Pooladian. An Explicit Expansion of the Kullback-Leibler Divergence along its Fisher-Rao Gradient Flow. *Transactions on Machine Learning Research*, 2023.
- [DH08] Fred Daum and Jim Huang. Particle flow for nonlinear filters with log-homotopy. In *Signal and Data Processing of Small Targets 2008*, volume 6969, pages 414–425. SPIE, 2008.
- [DHDS16] Bo Dai, Niao He, Hanjun Dai, and Le Song. Provable Bayesian inference via particle mirror descent. In *Artificial Intelligence and Statistics*, pages 985–994. PMLR, 2016.
- [DHJW22] Chenguang Dai, Jeremy Heng, Pierre E Jacob, and Nick Whiteley. An invitation to sequential Monte Carlo samplers. *Journal of the American Statistical Association*, 117(539):1587–1600, 2022.
- [DM97] Pierre Del Moral. Nonlinear filtering: Interacting particle resolution. *Comptes Rendus de l'Académie des Sciences - Series I - Mathematics*, 325(1):653–658, 1997.
- [dM04] Pierre del Moral. *Feynman-Kac formulae: genealogical and interacting particle systems with applications*. Probability and Its Applications. Springer Verlag, New York, 2004.
- [dMDJ06] Pierre del Moral, Arnaud Doucet, and Ajay Jasra. Sequential Monte Carlo samplers. *Journal of the Royal Statistical Society Series B: Statistical Methodology*, 68(3):411–436, 2006.
- [DMM19] Alain Durmus, Szymon Majewski, and Błażej Miasojedow. Analysis of Langevin Monte Carlo via convex optimization. *Journal of Machine Learning Research*, 20(73):1–46, 2019.
- [FA95] Akio Fujiwara and Shun-ichi Amari. Gradient systems in view of information geometry. *Physica D: Nonlinear Phenomena*, 80(3):317–327, 1995.
- [GCW19] Mathieu Gerber, Nicolas Chopin, and Nick Whiteley. Negative association, ordering and convergence of resampling methods. *Annals of Statistics*, 47(4):2236–2260, 2019.
- [Gey91] Charles J Geyer. Markov chain Monte Carlo maximum likelihood. In E. M. Keramides, editor, *Computing Science and Statistics: Proceedings of the 23rd Symposium on the Interface*, pages 156–163, 1991.
- [GIHLS20] Alfredo Garbuno-Inigo, Franca Hoffmann, Wuchen Li, and Andrew M Stuart. Interacting Langevin diffusions: Gradient structure and ensemble Kalman sampler. *SIAM Journal on Applied Dynamical Systems*, 19(1):412–441, 2020.
- [GM17] Thomas O Gallouët and Leonard Monsaingeon. A JKO splitting scheme for Kantorovich–Fisher–Rao gradient flows. *SIAM Journal on Mathematical Analysis*, 49(2):1100–1130, 2017.
- [GTC25] Wei Guo, Molei Tao, and Yongxin Chen. Provable benefit of annealed langevin monte carlo for non-log-concave sampling. In *The Thirteenth International Conference on Learning Representations*, 2025.
- [Har09a] Marc Harper. Information geometry and evolutionary game theory. *arXiv preprint arXiv:0911.1383*, 2009.
- [Har09b] Marc Harper. The replicator equation as an inference dynamic. *arXiv preprint arXiv:0911.1763*, 2009.
- [HS98] Josef Hofbauer and Karl Sigmund. *Evolutionary games and population dynamics*. Cambridge university press, 1998.

- [JKO98] Richard Jordan, David Kinderlehrer, and Felix Otto. The variational formulation of the Fokker–Planck equation. *SIAM Journal on Mathematical Analysis*, 29(1):1–17, 1998.
- [JSDT11] Ajay Jasra, David A Stephens, Arnaud Doucet, and Theodoros Tsagaris. Inference for Lévy-driven stochastic volatility models via adaptive sequential Monte Carlo. *Scandinavian Journal of Statistics*, 38(1):1–22, 2011.
- [KLJ23] Juan Kuntz, Jen Ning Lim, and Adam M Johansen. Particle algorithms for maximum likelihood training of latent variable models. *Proceedings of The 26th International Conference on Artificial Intelligence and Statistics*, 2023.
- [KP22] Anna Korba and François Portier. Adaptive importance sampling meets mirror descent: a bias-variance tradeoff. In *International Conference on Artificial Intelligence and Statistics*, pages 11503–11527. PMLR, 2022.
- [LCB⁺22] Marc Lambert, Sinho Chewi, Francis Bach, Silvère Bonnabel, and Philippe Rigollet. Variational inference via Wasserstein gradient flows. *Advances in Neural Information Processing Systems*, 35:14434–14447, 2022.
- [LLN19] Yulong Lu, Jianfeng Lu, and James Nolen. Accelerating Langevin Sampling with Birth-death. *arXiv preprint arXiv: 1905.09863*, pages 1–18, 2019.
- [LMTZ25] Matthias Liero, Alexander Mielke, Oliver Tse, and Jia-Jie Zhu. Evolution of Gaussians in the Hellinger-Kantorovich-Boltzmann gradient flow. *arXiv preprint arXiv:2504.20400*, 2025.
- [LSW23] Yulong Lu, Dejan Slepčev, and Lihan Wang. Birth-death dynamics for sampling: Global convergence, approximations and their asymptotics. *Nonlinearity*, 36(11):5731–5772, 2023.
- [LW16] Qiang Liu and Dilin Wang. Stein variational gradient descent: A general purpose Bayesian inference algorithm. *Advances in Neural Information Processing Systems*, 29, 2016.
- [MM24] Aimee Maurais and Youssef Marzouk. Sampling in unit time with kernel Fisher-rao flow. In Ruslan Salakhutdinov, Zico Kolter, Katherine Heller, Adrian Weller, Nuria Oliver, Jonathan Scarlett, and Felix Berkenkamp, editors, *Proceedings of the 41st International Conference on Machine Learning*, volume 235 of *Proceedings of Machine Learning Research*, pages 35138–35162. PMLR, 21–27 Jul 2024.
- [MMW⁺21] Wenlong Mou, Yi-An Ma, Martin J Wainwright, Peter L Bartlett, and Michael I Jordan. High-order Langevin diffusion yields an accelerated MCMC algorithm. *Journal of Machine Learning Research*, 22(1):1919–1959, 2021.
- [Nea01] Radford M Neal. Annealed importance sampling. *Statistics and Computing*, 11:125–139, 2001.
- [Nüs24] Nikolas Nüsken. Stein Transport for Bayesian Inference. *arXiv preprint arXiv:2409.01464*, 2024.
- [NVPB24] Nikolas Nüsken, Francisco Vargas, Shreyas Padhy, and Denis Blessing. Transport Meets Variational Inference: Controlled Monte Carlo Diffusions. In *The Twelfth International Conference on Learning Representations: ICLR 2024*, 2024.
- [PHHV23] Benjamin Pampel, Simon Holbach, Lisa Hartung, and Omar Valsson. Sampling rare event energy landscapes via birth-death augmented dynamics. *Physical Review E*, 107(2):024141, 2023.
- [PW24] Sahani Pathiraja and Philipp Wacker. Connections between sequential Bayesian inference and evolutionary dynamics. *Philosophical Transactions of the Royal Society A: Mathematical, Physical and Engineering Sciences (accepted)*, 2024.
- [RS02] Gareth O Roberts and Osnat Stramer. Langevin Diffusions and Metropolis-Hastings Algorithms. *Methodology and Computing in Applied Probability*, 4, 2002.

- [RT96] Gareth O Roberts and Richard L Tweedie. Exponential convergence of Langevin distributions and their discrete approximations. *Bernoulli*, pages 341–363, 1996.
- [SBCCD24] Saifuddin Syed, Alexandre Bouchard-Côté, Kevin Chern, and Arnaud Doucet. Optimised annealed sequential Monte Carlo samplers. *arXiv preprint arXiv:2408.12057*, 2024.
- [Sch19] André Schlichting. Poincaré and log–Sobolev inequalities for mixtures. *Entropy*, 21(1):89, 2019.
- [Sha09] Cosma Rohilla Shalizi. Dynamics of bayesian updating with dependent data and misspecified models. *Electronic Journal of Statistics*, 3:1039–1074, 2009.
- [SKL20] Adil Salim, Anna Korba, and Giulia Luise. The Wasserstein proximal gradient algorithm. *Advances in Neural Information Processing Systems*, 33:12356–12366, 2020.
- [VW19] Santosh Vempala and Andre Wibisono. Rapid convergence of the unadjusted Langevin algorithm: Isoperimetry suffices. *Advances in neural information processing systems*, 32, 2019.
- [Wib18] Andre Wibisono. Sampling as optimization in the space of measures: The Langevin dynamics as a composite optimization problem. In *Conference on Learning Theory*, pages 2093–3027. PMLR, 2018.
- [WN24] Linfeng Wang and Nikolas Nüsken. Measure transport with kernel mean embeddings. *arXiv preprint arXiv:2401.12967*, pages 1–21, 2024.
- [YWR24] Yuling Yan, Kaizheng Wang, and Philippe Rigollet. Learning Gaussian mixtures using the Wasserstein–Fisher–Rao gradient flow. *Annals of Statistics*, 52(4):1774–1795, 2024.

A Supplementary Lemmata

Lemma A.1. Let ρ_t denote an unnormalised probability density function, and assume its time evolution is governed by

$$\partial_t \rho_t(x) = \rho_t(x) f(x) \quad (\text{A.1})$$

for some function $f(x)$, also known as the “fitness function” in the evolutionary biology literature. The evolution of the normalised probability density $\mu_t(x) = \frac{\rho_t(x)}{\int \rho_t(y) dy}$ is given by the replicator PDE

$$\partial_t \mu_t(x) = \mu_t(x) (f(x) - \mathbb{E}_{\mu_t}[f]) \quad (\text{A.2})$$

Proof. Differentiating the expression for $\mu_t(x)$ with respect to t and substituting in (A.1),

$$\begin{aligned} \partial_t \mu_t(x) &= \frac{\partial_t \rho_t(x)}{\int \rho_t(y) dy} - \frac{\rho_t(x)}{(\int \rho_t(y) dy)^2} \int \partial_t \rho_t(y) dy \\ &= \frac{\rho_t(x) f(x)}{\int \rho_t(y) dy} - \frac{\rho_t(x)}{(\int \rho_t(y) dy)^2} \int f(y) \rho_t(y) dy \\ &= \mu_t(x) f(x) - \mu_t(x) \int f(y) \mu_t(y) dy \end{aligned}$$

yields the desired result. \square

Lemma A.2 (Unit time FR as a deterministic time rescaling of infinite time FR.). Consider the unit time FR PDE

$$\partial_t \mu_t(x) = \mu_t(x) \log \left(\frac{\pi(x)}{\mu_0(x)} \right) - \mathbb{E}_{\mu_t} \left[\frac{\pi(x)}{\mu_0(x)} \right], \quad t \in [0, 1] \quad (\text{A.3})$$

Let $\mu_\tau^* = \mu_t$ where $\tau = -\log(1-t)$ and μ_t is a solution of (A.3). Then formally, μ_τ^* is a solution of the infinite time FR PDE

$$\partial_t \mu_\tau^*(x) = \mu_\tau^*(x) \log \left(\frac{\pi(x)}{\mu_\tau^*(x)} \right) - \mathbb{E}_{\mu_\tau^*} \left[\frac{\pi(x)}{\mu_\tau^*(x)} \right], \quad \tau \in [0, \infty)$$

Proof. Consider the geometric interpolation

$$\rho_t(x) = \pi^t(x) \rho_0^{1-t}(x) = \exp[t \log \pi(x) + (1-t) \log \rho_0(x)] \quad (\text{A.4})$$

where ρ_t denotes an unnormalised probability density. Differentiating both sides with respect to t yields

$$\partial_t \rho_t = \rho_t(x) \log \left(\frac{\pi(x)}{\rho_0(x)} \right), \quad t \in [0, 1], \quad (\text{A.5})$$

that is, the unit time Fisher–Rao PDE in unnormalised form (see Lemma A.1). Consider the deterministic time change $\tau = -\log(1-t)$ where $\tau \in [0, \infty)$ such that $\rho_\tau^* = \rho_t$. Then using (A.4),

$$\log \rho_\tau^* = \log \rho_{t(\tau)} = (1 - \exp(-\tau)) \log \pi + \exp(-\tau) \log \rho_0 \quad (\text{A.6})$$

and $\frac{dt}{d\tau} = \exp(-\tau)$. Combining these results and applying chain rule to (A.5),

$$\begin{aligned} \partial_\tau \rho_\tau^* &= \frac{dt}{d\tau} \partial_t \rho_{t(\tau)} = \exp(-\tau) \rho_{t(\tau)} \log \left(\frac{\pi}{\rho_0} \right) \\ &= \rho_{t(\tau)} [\exp(-\tau) \log \pi - \exp(-\tau) \log \rho_0] \\ &= \rho_\tau^* [\exp(-\tau) \log \pi - \exp(-\tau) \log \rho_0] \\ &= \rho_\tau^* [\exp(-\tau) \log \pi + (1 - \exp(-\tau)) \log \pi - \log \rho_\tau^*] \\ &= \rho_\tau^* [\log \pi - \log \rho_\tau^*] \end{aligned}$$

yields the unnormalised form of the infinite time FR PDE. Applying the normalisation Lemma A.1 yields the result. \square

B Convergence Results

B.1 Convergence of Continuous Time Schemes

B.1.1 Wasserstein Fisher Rao Flow

We consider the time derivative of $D_{\text{KL}}(\mu_t|\pi)$ along the WFR flow

$$\frac{d}{dt}D_{\text{KL}}(\mu_t|\pi) = \int \log \frac{\mu_t}{\pi} \partial_t \mu_t = - \int \mu_t \|\nabla \log \frac{\mu_t}{\pi}\|^2 - \int \mu_t \left(\log \frac{\mu_t}{\pi} \right)^2 + D_{\text{KL}}(\mu_t|\pi)^2.$$

If π satisfies a Log-Sobolev inequality with constant C_{LSI} and $\inf_{x \in \mathbb{R}^d} \frac{\mu_0(x)}{\pi(x)} \geq e^{-M}$, using the proof strategy of [LLN19, Theorem 3.2] we find

$$\frac{d}{dt}D_{\text{KL}}(\mu_t|\pi) \leq -2C_{\text{LSI}}^{-1}D_{\text{KL}}(\mu_t|\pi) - (2 - 2\delta)D_{\text{KL}}(\mu_t|\pi) + D_{\text{KL}}(\mu_t|\pi)^2,$$

for some $\delta > 0$ and $t \geq |\log(\delta/M)|$. Further assuming that $D_{\text{KL}}(\mu_0|\pi) \leq 1$ and using [LLN19, Eq. (B.7)] we have

$$\frac{d}{dt}D_{\text{KL}}(\mu_t|\pi) \leq -(2C_{\text{LSI}}^{-1} + (2 - 3\delta))D_{\text{KL}}(\mu_t|\pi),$$

$t \geq t_0 := \log(M/\delta^3)$. Applying Grönwall's Lemma we obtain

$$D_{\text{KL}}(\mu_t|\pi) \leq e^{-(2C_{\text{LSI}}^{-1} + (2 - 3\delta))(t - t_0)}D_{\text{KL}}(\mu_0|\pi),$$

showing that combining W with FR improves the convergence rate.

B.1.2 Tempered Wasserstein PDE

Consider the W PDE

$$\partial_t \mu_t = \nabla \cdot \left(\mu_t \nabla \log \left(\frac{\mu_t}{\pi_t} \right) \right)$$

where $\pi_t \propto \pi^{\lambda_t} \mu_0^{1-\lambda_t}$ and $\lambda_t : \mathbb{R}_+ \rightarrow [0, 1]$, λ_t is non-decreasing in t and weakly differentiable.

A direct computation of the decay of $D_{\text{KL}}(\mu_t|\pi)$ along this PDE gives

$$\begin{aligned} \frac{d}{dt}D_{\text{KL}}(\mu_t|\pi) &= - \int \mu_t \|\nabla \log \frac{\mu_t}{\pi}\|^2 + (1 - \lambda_t) \int \log \frac{\mu_t}{\pi} \nabla \cdot \left(\mu_t \nabla \log \left(\frac{\pi}{\mu_0} \right) \right) \\ &= - \int \mu_t \|\nabla \log \frac{\mu_t}{\pi}\|^2 + (1 - \lambda_t) \int \mu_t [\Delta V_{\mu_0} - \Delta V_{\pi} - \langle \nabla V_{\pi}, \nabla V_{\mu_0} - \nabla V_{\pi} \rangle] \end{aligned}$$

where we used the expression for π_t and multiple applications of integrations by parts.

To proceed we recall that Assumption 1 implies the dissipativity condition

$$\langle x, \nabla V_{\pi}(x) \rangle \geq a_{\pi} \|x\|^2 - b_{\pi}, \tag{B.1}$$

with $a_{\pi} = c_{\pi} - 1/(2\epsilon) > 0$ and $b_{\pi} = \epsilon \|\nabla V_{\pi}(0)\|^2/2 > 0$ for $\epsilon > 1/(2c_{\pi})$ (see, e.g., [CDDJ24, Appendix B.3] for a proof). A consequence of the dissipativity (B.1) is

$$\mathbb{E}_{\pi}[\|X\|^2] \leq \frac{1}{a_{\pi}} \mathbb{E}_{\pi}[\langle X, \nabla V_{\pi}(X) \rangle] + \frac{b_{\pi}}{a_{\pi}} = \frac{d + b_{\pi}}{a_{\pi}}. \tag{B.2}$$

In addition, V_{π} must be minimised at some point $z_0 \in B(0, \sqrt{\frac{b_{\pi}}{a_{\pi}}})$, thus the Lipschitz assumption implies

$$\|\nabla V_{\pi}(z)\|^2 \leq 2L_{\pi}^2 \left(\|z\|^2 + \frac{b_{\pi}}{a_{\pi}} \right). \tag{B.3}$$

The same properties follow from Assumption 2 for μ_0 .

Using the above and [CKSV25, Lemma 15] we have

$$\begin{aligned}
& \int \mu_t [\Delta V_{\mu_0} - \Delta V_\pi - \langle \nabla V_\pi, \nabla V_{\mu_0} - \nabla V_\pi \rangle] \\
& \leq d(L_{\mu_0} - c_\pi) + 2L_\pi^2 \left(\mathbb{E}_{\mu_t} [\|x\|^2] + \frac{b_\pi}{a_\pi} \right) + \int \mu_t (\|\nabla V_\pi\|^2 \vee \|\nabla V_{\mu_0}\|^2) \\
& \leq d(L_{\mu_0} - c_\pi) + 4(L_\pi^2 \vee L_{\mu_0}^2) \left(\mathbb{E}_{\mu_t} [\|x\|^2] + \left(\frac{b_\pi}{a_\pi} \vee \frac{b_0}{a_0} \right) \right) \\
& \leq d(L_{\mu_0} - c_\pi) + 4(L_\pi^2 \vee L_{\mu_0}^2) \left(\mathbb{E}_{\mu_0} [\|x\|^2] \vee \frac{d + b_{\mu_0} + b_\pi}{a_{\mu_0} \wedge a_\pi} + \left(\frac{b_\pi}{a_\pi} \vee \frac{b_0}{a_0} \right) \right) := A.
\end{aligned}$$

Using Grönwall's Lemma we obtain

$$D_{\text{KL}}(\mu_t | | \pi) \leq e^{-2tC_{\text{LSI}}^{-1}} D_{\text{KL}}(\mu_0 | | \pi) + A \int_0^t e^{-2(t-s)C_{\text{LSI}}^{-1}} (1 - \lambda_s) ds,$$

with $C_{\text{LSI}} = c_\pi^{-1}$.

B.1.3 Tempered Fisher Rao PDE

Consider the FR PDE

$$\partial_t \mu_t = \mu_t(x) \left(\log \left(\frac{\pi_t(x)}{\mu_t(x)} \right) - \mathbb{E}_{\mu_t} \left[\log \left(\frac{\pi_t}{\mu_t} \right) \right] \right),$$

where $\pi_t \propto \pi^{\lambda_t} \mu_0^{1-\lambda_t}$ and $\lambda_t : \mathbb{R}_+ \rightarrow [0, 1]$, λ_t is non-decreasing in t and weakly differentiable. Using an argument similar to that of [CHH⁺23b, Appendix B.1] we can show that this PDE reduces the Kullback–Leibler divergence w.r.t. π .

Using the fact that

$$\frac{\partial e^t \log \mu_t(x)}{\partial t} = e^t \log \pi_t(x) - e^t \mathbb{E}_{\mu_t} \left[\log \left(\frac{\pi_t}{\mu_t} \right) \right]$$

and the expression for π_t we have

$$\log \mu_t(x) = \log \mu_0(x) \left(\int e^{s-t}(1 - \lambda_s) ds + e^{-t} \right) + \log \pi(x) \int e^{s-t} \lambda_s ds - \int_0^t e^{s-t} \mathbb{E}_{\mu_s} \left[\log \left(\frac{\pi_s}{\mu_s} \right) \right] ds.$$

It follows that

$$\mu_t \propto \mu_0^{e^{-t} + \int_0^t e^{s-t}(1-\lambda_s) ds} \pi^{\int_0^t e^{s-t} \lambda_s ds}. \quad (\text{B.4})$$

The normalising constant of μ_t satisfies

$$\begin{aligned}
Z_t & := \int \mu_0(x)^{1 - \int_0^t e^{s-t} \lambda_s ds} \pi(x)^{\int_0^t e^{s-t} \lambda_s ds} dx \\
& = \int \pi(x) \left(\frac{\pi(x)}{\mu_0(x)} \right)^{1 - \int_0^t e^{s-t} \lambda_s ds} dx \\
& \geq \int \pi(x) \exp \left(-M(1 + \|x\|^2) \left(1 - \int_0^t e^{s-t} \lambda_s ds \right) \right) dx \\
& \geq \exp \left(\int \pi(x) \left(-M(1 + \|x\|^2) \left(1 - \int_0^t e^{s-t} \lambda_s ds \right) \right) dx \right) \\
& \geq \exp \left(-M(1 + B) \left(1 - \int_0^t e^{s-t} \lambda_s ds \right) \right),
\end{aligned}$$

where we used (2.7) and Jensen's inequality.

Since $\int_0^t e^{s-t} \lambda_s ds < 1$ we also have

$$\begin{aligned} \frac{\mu_t(x)}{\pi(x)} &= \frac{1}{Z_t} \frac{\mu_0(x)^{1-\int_0^t e^{s-t} \lambda_s ds} \pi(x)^{\int_0^t e^{s-t} \lambda_s ds}}{\pi(x)} \\ &= \frac{1}{Z_t} \left(\frac{\mu_0(x)}{\pi(x)} \right)^{1-\int_0^t e^{s-t} \lambda_s ds} \\ &\leq \exp \left(M(1+B)(1-\int_0^t e^{s-t} \lambda_s ds) + M(1+\|x\|^2)(1-\int_0^t e^{s-t} \lambda_s ds) \right) \end{aligned}$$

from which we obtain the result

$$\begin{aligned} D_{\text{KL}}(\mu_t|\pi) &\leq M(1+B)(1-\int_0^t e^{s-t} \lambda_s ds) + M(1+\int \mu_t(x)\|x\|^2 dx)(1-\int_0^t e^{s-t} \lambda_s ds) \\ &\leq M(1+B)(1-\int_0^t e^{s-t} \lambda_s ds) + M(1+B \exp \left(M(1+B)(1-\int_0^t e^{s-t} \lambda_s ds) \right))(1-\int_0^t e^{s-t} \lambda_s ds) \end{aligned}$$

using Proposition B.1.

Proposition B.1. *Assume that $\int \|x\|^2 \mu_0(x) dx \leq B$, $\int \|x\|^2 \pi(x) dx \leq B$ and (2.7), then*

$$\int \mu_t(x)\|x\|^2 dx \leq B \exp \left(M(1+B)(1-\int_0^t e^{s-t} \lambda_s ds) \right).$$

Proof. Using the expression for μ_t in (B.4) and Hölder inequality with $p = (1-\int_0^t e^{s-t} \lambda_s ds)^{-1}$ and $q = (\int_0^t e^{s-t} \lambda_s ds)^{-1}$ gives

$$\begin{aligned} \int \mu_t(x)\|x\|^2 dx &= \frac{1}{Z_t} \int (\mu_0(x)\|x\|^2)^{1-\int_0^t e^{s-t} \lambda_s ds} (\pi(x)\|x\|^2)^{\int_0^t e^{s-t} \lambda_s ds} dx \\ &\leq \frac{1}{Z_t} \left(\int \mu_0(x)\|x\|^2 dx \right)^{1-\int_0^t e^{s-t} \lambda_s ds} \left(\int \pi(x)\|x\|^2 dx \right)^{\int_0^t e^{s-t} \lambda_s ds} \\ &\leq B \exp \left(M(1+B)(1-\int_0^t e^{s-t} \lambda_s ds) \right). \end{aligned}$$

□

B.1.4 Tempered Wasserstein Fisher Rao PDE

As in the case of the other tempered PDEs, we consider the decay of $D_{\text{KL}}(\mu|\pi)$ along the flow described by (2.15):

$$\begin{aligned} \frac{d}{dt} D_{\text{KL}}(\mu_t|\pi) &= \int \log \frac{\mu_t}{\pi} \nabla \cdot \left(\mu_t \nabla \log \left(\frac{\mu_t}{\pi_t} \right) \right) + \int \mu_t \log \frac{\mu_t}{\pi} \log \frac{\pi_t}{\mu_t} - D_{\text{KL}}(\mu_t|\pi) \mathbb{E}_{\mu_t} \left[\log \left(\frac{\pi_t}{\mu_t} \right) \right] \\ &= - \int \mu_t \|\nabla \log \frac{\mu_t}{\pi}\|^2 - \text{var}_{\mu_t} \left(\log \frac{\mu_t}{\pi} \right) \\ &\quad + (1-\lambda_t) \left[\int \log \frac{\mu_t}{\pi} \nabla \cdot \left(\mu_t \nabla \log \left(\frac{\pi}{\mu_0} \right) \right) - \text{cov}_{\mu_t} \left(\log \frac{\mu_t}{\pi}, \log \frac{\pi}{\mu_0} \right) \right], \end{aligned}$$

where we used the expression for π_t and multiple applications of integrations by parts.

We recognise the derivative of the standard WFR flow in the first term, the second term is due to the use of the tempered targets π_t and in fact is 0 for $\lambda_t \equiv 1$. By defining the derivative of $D_{\text{KL}}(\mu|\pi)$ along the tempered W flow (2.12) and that along the tempered FR flow (2.14)

$$\begin{aligned} \frac{d}{dt} D_{\text{KL}}(\mu_t^{\text{T-W}}|\pi) &:= - \int \mu_t \|\nabla \log \frac{\mu_t}{\pi}\|^2 + (1-\lambda_t) \int \log \frac{\mu_t}{\pi} \nabla \cdot \left(\mu_t \nabla \log \left(\frac{\pi}{\mu_0} \right) \right) \\ \frac{d}{dt} D_{\text{KL}}(\mu_t^{\text{T-FR}}|\pi) &:= - \text{var}_{\mu_t} \left(\log \frac{\mu_t}{\pi} \right) - (1-\lambda_t) \text{cov}_{\mu_t} \left(\log \frac{\mu_t}{\pi}, \log \frac{\pi}{\mu_0} \right) \end{aligned}$$

we can write

$$\frac{d}{dt}D_{\text{KL}}(\mu_t^{\text{T-WFR}}|\pi) = \frac{d}{dt}D_{\text{KL}}(\mu_t^{\text{T-W}}|\pi) + \frac{d}{dt}D_{\text{KL}}(\mu_t^{\text{T-FR}}|\pi),$$

showing that the W and FR geometries are indeed orthogonal as shown in [GM17].

It follows that

$$D_{\text{KL}}(\mu_t^{\text{T-WFR}}|\pi) \leq \min \{D_{\text{KL}}(\mu_t^{\text{T-W}}|\pi), D_{\text{KL}}(\mu_t^{\text{T-FR}}|\pi)\}.$$

B.1.5 Gradient flow structure of tempered PDEs

The tempered PDEs described above do not correspond to gradient flows of $D_{\text{KL}}(\mu|\pi)$. To identify a gradient flow structure, we consider the functional $\mathcal{F}(\mu, \lambda) : \mathcal{P}(\mathbb{R}^d) \times [0, 1] \rightarrow \mathbb{R}$ defined as $\mathcal{F}(\mu, \lambda) := D_{\text{KL}}(\mu|\pi_\lambda)$ where optimisation occurs both on μ and on λ , whose evolution satisfies

$$\dot{\lambda}_t = \int \mu_t \log \frac{\pi}{\mu_0} - \int \pi_t \log \frac{\pi}{\mu_0}. \quad (\text{B.5})$$

Gradient flows on joint spaces have been recently considered by [CKPJ25, KLJ23] which establish conditions on \mathcal{F} to guarantee convergence of the corresponding Wasserstein gradient flow. Under the assumption that both μ_0 and π are strongly log-concave (see Assumption 1 and 2 below), [CKPJ25, Theorem 1] guarantees that the Wasserstein gradient flow of \mathcal{F} given by (2.12) and (B.5) converges exponentially:

$$0 \leq \mathcal{F}(\mu_t, \lambda_t) \leq \mathcal{F}(\nu, \lambda_0) e^{-2t(c_{\mu_0} \wedge c_\pi)} \quad (\text{B.6})$$

where c_{μ_0}, c_π denote the convexity constants of μ_0, π , respectively, and ν is the initial condition of (2.12) (see Appendix B.1 for a proof).

To apply [CKPJ25, Theorem 1] we check Assumption 1 and 2 therein as well as the extended log-Sobolev inequality (Eq. (11) therein).

The mapping $\lambda \mapsto \pi_\lambda = \mu_0^{1-\lambda} \pi^\lambda / Z_\lambda$ is twice continuously differentiable with derivatives

$$\partial_\lambda \log \pi_\lambda(x) = \log \frac{\pi(x)}{\mu_0(x)} - \int \pi_\lambda \log \frac{\pi(x)}{\mu_0(x)}, \quad \partial_\lambda^2 \log \pi_\lambda(x) = \text{var}_{\pi_\lambda} \left(\frac{\pi}{\mu_0} \right)$$

which are finite quantities under Assumption 1 and 2. In addition, $\pi_\lambda(x) > 0$ for all λ, x if $\mu_0(x) > 0$ and $\pi(x) > 0$. The Lipschitz continuity in Assumption 1 and 2 then guarantees that [CKPJ25, Assumption 2] is satisfied.

To check the extended log-Sobolev inequality in [CKPJ25, Eq. (11)] we note that $\mathcal{F}^* = 0$ and, since π_λ is strongly log-concave under Assumption 1 and 2,

$$\mathcal{F}(\mu, \lambda) = D_{\text{KL}}(\mu|\pi_\lambda) \leq \frac{1}{2c_\lambda} \int \|\nabla_x \log \frac{\mu(x)}{\pi_\lambda(x)}\|^2 \mu(x) dx \leq \frac{1}{2(c_{\mu_0} \wedge c_\pi)} \int \|\nabla_x \log \frac{\mu(x)}{\pi_\lambda(x)}\|^2 \mu(x) dx$$

where $c_\lambda \geq (1-\lambda)c_{\mu_0} + \lambda c_\pi \geq c_{\mu_0} \wedge c_\pi$ is the convexity constant of π_λ .

B.2 Convergence of Discrete Time Schemes

B.2.1 Proof of Proposition 3.1

Proof. Let us denote $\mathcal{F}(\mu) = D_{\text{KL}}(\mu|\pi)$. To show that the mirror descent update (3.5) reduces \mathcal{F} we reproduce the argument of [CCK24, Proposition 1]. Since \mathcal{F} is 1-relatively smooth with respect to $\phi : \mu \mapsto \int \log(\mu(x)) d\mu(x)$ [AFKL22] and since $\delta = 1 - e^{-\gamma} \leq 1$, for all $\gamma > 0$, we have

$$\begin{aligned} \mathcal{F}(\mu_n) &\leq \mathcal{F}(\mu_{n-1/2}) + \langle \nabla \mathcal{F}(\mu_{n-1/2}), \mu_n - \mu_{n-1/2} \rangle + B_\phi(\mu_n|\mu_{n-1/2}) \\ &\leq \mathcal{F}(\mu_{n-1/2}) + \langle \nabla \mathcal{F}(\mu_{n-1/2}), \mu_n - \mu_{n-1/2} \rangle + \frac{1}{\delta} B_\phi(\mu_n|\mu_{n-1/2}), \end{aligned} \quad (\text{B.7})$$

where $B_\phi(\nu|\mu) = \phi(\nu) - \phi(\mu) - \langle \nabla\phi(\mu), \nu - \mu \rangle$ denotes the Bregman divergence and $\nabla\phi$ the first variation. Applying [AFKL22, Lemma 3] to the convex function $G(\nu) = \delta \langle \nabla\mathcal{F}(\mu_{n-1/2}), \nu - \mu_{n-1/2} \rangle$, with $\mu = \mu_{n-1/2}$ and $\bar{\nu} = \mu_n$ yields

$$\begin{aligned} \langle \nabla\mathcal{F}(\mu_{n-1/2}), \mu_n - \mu_{n-1/2} \rangle + \frac{1}{\delta} B_\phi(\mu_n|\mu_{n-1/2}) &\leq \\ \langle \nabla\mathcal{F}(\mu_{n-1}), \nu - \mu_{n-1/2} \rangle + \frac{1}{\delta} B_\phi(\nu|\mu_{n-1/2}) - \frac{1}{\delta} B_\phi(\nu|\mu_n). \end{aligned}$$

Fix ν , then (B.7) becomes:

$$\mathcal{F}(\mu_n) \leq \mathcal{F}(\mu_{n-1/2}) + \langle \nabla\mathcal{F}(\mu_{n-1/2}), \nu - \mu_{n-1/2} \rangle + \frac{1}{\delta} B_\phi(\nu|\mu_{n-1/2}) - \frac{1}{\delta} B_\phi(\nu|\mu_n).$$

This shows in particular, by substituting $\nu = \mu_{n-1/2}$ and since $B_\phi(\nu|\mu_n) \geq 0$, that

$$\mathcal{F}(\mu_n) \leq \mathcal{F}(\mu_{n-1/2}) - \frac{1}{\delta} B_\phi(\mu_{n-1/2}|\mu_n). \quad (\text{B.8})$$

To deal with the W flow update we observe that $\mu_{n-1/2}$ in (3.4) with fixed is obtained as

$$\mu_{n-1/2}(x) = \mu_{n-1} R_\gamma(x) := (4\pi\gamma)^{-d/2} \int \exp\left(-\frac{1}{4\gamma} \|x - y - \gamma \nabla \log \pi(y)\|^2\right) \mu_{n-1}(y) dy$$

and using [VW19, Lemma 3]

$$\mathcal{F}(\mu_{n-1/2}) \leq e^{-\gamma/C_{\text{LSI}}} \mathcal{F}(\mu_{n-1}) + 6\gamma^2 dL_\pi^2,$$

with $\gamma \leq C_{\text{LSI}}^{-1}/(4L_\pi^2)$. Using (B.8), the result above and the fact that $B_\phi \geq 0$ we obtain

$$\mathcal{F}(\mu_n) \leq e^{-\gamma/C_{\text{LSI}}} \mathcal{F}(\mu_{n-1}) + 6\gamma^2 dL_\pi^2.$$

Proceeding by induction we then find that

$$\begin{aligned} \mathcal{F}(\mu_n) &\leq e^{-n\gamma/C_{\text{LSI}}} \mathcal{F}(\mu_0) + 6\gamma^2 dL_\pi^2 \sum_{k=0}^{n-1} e^{-k\gamma/C_{\text{LSI}}} \\ &\leq e^{-n\gamma/C_{\text{LSI}}} \mathcal{F}(\mu_0) + 6\gamma^2 dL_\pi^2 \left(\frac{1 - e^{-(n-1)\gamma/C_{\text{LSI}}}}{1 - e^{-\gamma/C_{\text{LSI}}}} \right) \\ &\leq e^{-n\gamma/C_{\text{LSI}}} \mathcal{F}(\mu_0) + 6\gamma^2 dL_\pi^2 \left(\frac{1}{1 - e^{-\gamma/C_{\text{LSI}}}} \right) \\ &\leq e^{-n\gamma/C_{\text{LSI}}} \mathcal{F}(\mu_0) + 8\gamma dL_\pi^2 C_{\text{LSI}}^{-1}, \end{aligned}$$

where for the last inequality we used the fact that $\gamma \leq C_{\text{LSI}}^{-1}/(4L_\pi^2) \leq C_{\text{LSI}}/4$ as in [VW19, Theorem 1]. \square

B.2.2 Proof of Proposition 3.2

Proof. Let us denote $\mathcal{F}(\mu) = D_{\text{KL}}(\mu|\pi)$. We start by observing that the exact solution of tempered FR flow (3.8) corresponds to a mirror descent update (3.5) with $\delta_n = \int_0^{\gamma_n} e^{s-\gamma_n} \lambda_s ds \leq 1$. We can therefore use the same result in the previous proof to obtain

$$\mathcal{F}(\mu_n) \leq \mathcal{F}(\mu_{n-1/2}) - \frac{1}{\delta_n} B_\phi(\mu_{n-1/2}|\mu_n) \leq \mathcal{F}(\mu_{n-1/2}). \quad (\text{B.9})$$

To deal with the tempered W flow update we use Step 2 in the proof of [CKSV25, Theorem 3] to obtain

$$\mathcal{F}(\mu_{n-1/2}) = D_{\text{KL}}(\mu_{n-1/2}|\pi_n) + \int \mu_{n-1/2}(x) \log \frac{\pi_n(x)}{\pi(x)} dx. \quad (\text{B.10})$$

Following a similar strategy as above, we observe that $\mu_{n-1/2}$ in (3.7) is obtained as

$$\mu_{n-1/2}(x) = \mu_{n-1}R_{\gamma_n}(x) := (4\pi\gamma_n)^{-d/2} \int \exp\left(-\frac{1}{4\gamma_n}\|x-y-\gamma_n\nabla\log\pi_n(y)\|^2\right) \mu_{n-1}(y)dy \quad (\text{B.11})$$

and using [VW19, Lemma 3] with $\gamma_n \leq c_{\pi_n}/(4L_{\pi_n}^2)$ we obtain

$$D_{\text{KL}}(\mu_{n-1/2}||\pi_n) \leq e^{-\gamma_n c_{\pi_n}} D_{\text{KL}}(\mu_{n-1}||\pi_n) + 6\gamma_n^2 dL_{\pi_n}^2.$$

Using (B.9), (B.10) and the result above we obtain

$$\begin{aligned} \mathcal{F}(\mu_n) &\leq e^{-\gamma_n c_{\pi_n}} D_{\text{KL}}(\mu_{n-1}||\pi_n) + 6\gamma_n^2 dL_{\pi_n}^2 + \int \mu_{n-1/2}(x) \log \frac{\pi_n(x)}{\pi(x)} dx \\ &\leq e^{-\gamma_n c_{\pi_n}} \mathcal{F}(\mu_{n-1}) + 6\gamma_n^2 dL_{\pi_n}^2 + \int [\mu_{n-1}(x) - \mu_{n-1/2}(x)] \log \frac{\pi(x)}{\pi_n(x)} dx \\ &= e^{-\gamma_n c_{\pi_n}} \mathcal{F}(\mu_{n-1}) + 6\gamma_n^2 dL_{\pi_n}^2 + (1-\lambda_n) \int [\mu_{n-1}(x) - \mu_{n-1/2}(x)] \log \frac{\pi(x)}{\mu_0(x)} dx, \end{aligned}$$

where we used the fact that $D_{\text{KL}}(\mu_{n-1}||\pi_n) = D_{\text{KL}}(\mu_{n-1}||\pi) + \int \mu_{n-1} \log \pi/\pi_n$ and $e^{-\gamma_n c_{\pi_n}} \leq 1$ and that $\pi_n = \mu_0^{1-\lambda_n} \pi^{\lambda_n} / \mathcal{Z}_n$.

Applying Lemma B.2 we obtain

$$\begin{aligned} \mathcal{F}(\mu_n) &\leq e^{-\gamma_n c_{\pi_n}} \mathcal{F}(\mu_{n-1}) + 6\gamma_n^2 dL_{\pi_n}^2 + (1-\lambda_n) \int [\mu_{n-1}(x) - \mu_{n-1/2}(x)] \log \frac{\pi(x)}{\mu_0(x)} dx \\ &\leq e^{-\gamma_n c_{\pi_n}} \mathcal{F}(\mu_{n-1}) + 6\gamma_n^2 dL_{\pi_n}^2 + 2\gamma_n(1-\lambda_n)(A + B\mathbb{E}_{\mu_{n-1}}[\|Y\|^2]) \end{aligned}$$

where A, B are given in Lemma B.2. Finally, using the moment bound in Lemma B.3 we find

$$\begin{aligned} \mathcal{F}(\mu_n) &\leq e^{-\gamma_n c_{\pi_n}} \mathcal{F}(\mu_{n-1}) + 6\gamma_n^2 dL_{\pi_n}^2 + 2\gamma_n(1-\lambda_n)A \\ &\quad + 2\gamma_n(1-\lambda_n)B\mathbb{E}_{\mu_0}[\|X\|^2] \left(\frac{d+b_\pi}{a_\pi}\right)^{\sum_{k=1}^{n-1} \delta_k} \prod_{k=1}^{n-1} Z_k^{-1} \\ &\quad + 4\gamma_n(1-\lambda_n)B(d+2(b_\pi \vee b_{\mu_0})) \sum_{k=1}^{n-1} \gamma_k \left(\frac{d+b_\pi}{a_\pi}\right)^{\sum_{i=k}^{n-1} \delta_i} \prod_{i=k}^{n-1} Z_i^{-1}. \end{aligned}$$

Using induction we then obtain

$$\begin{aligned} \mathcal{F}(\mu_n) &\leq \mathcal{F}(\mu_0) e^{-\sum_{k=1}^n \gamma_k c_{\pi_k}} + \sum_{k=0}^{n-1} (6\gamma_k^2 dL_{\pi_k}^2 + 2\gamma_k(1-\lambda_k)A) e^{-\sum_{i=1}^k \gamma_i c_{\pi_i}} \\ &\quad + \sum_{k=0}^{n-1} 2\gamma_k(1-\lambda_k)B\mathbb{E}_{\mu_0}[\|X\|^2] e^{-\sum_{i=1}^k \gamma_i c_{\pi_i}} \left(\frac{d+b_\pi}{a_\pi}\right)^{\sum_{j=1}^{k-1} \delta_j} \prod_{j=1}^{n-1} Z_j^{-1} \\ &\quad + \sum_{k=0}^{n-1} 4\gamma_k(1-\lambda_k)B(d+2(b_\pi \vee b_{\mu_0})) e^{-\sum_{i=1}^k \gamma_i c_{\pi_i}} \sum_{j=1}^{k-1} \gamma_j \left(\frac{d+b_\pi}{a_\pi}\right)^{\sum_{i=j}^{k-1} \delta_i} \prod_{i=j}^{k-1} Z_i^{-1}. \end{aligned}$$

□

B.2.3 Auxiliary results for the proof of Proposition 3.2

Under Assumption 2 and Assumption 1, we have that $\pi_n = \pi_{\lambda_n} = \pi_{\lambda_{t_n}}$ satisfies $\nabla V_{\pi_n} := (1-\lambda_n)\nabla V_{\mu_0} + \lambda_n\nabla V_\pi$ is Lipschitz continuous with Lipschitz constant $L_{\pi_n} = (1-\lambda_n)L_{\mu_0} + \lambda_n L_\pi$ and strongly convex with constant $c_{\pi_n} = (1-\lambda_n)c_{\mu_0} + \lambda_n c_\pi$. Using (B.1) and recalling that the same condition holds true for μ_0 with constants a_{μ_0}, b_{μ_0} , we have

$$\langle x, \nabla V_{\pi_n}(x) \rangle \geq a_{\pi_n} \|x\|^2 - b_{\pi_n}, \quad (\text{B.12})$$

with $a_{\pi_n} = \lambda_n a_\pi + (1 - \lambda_n) a_{\mu_0} > 0$ and $b_{\pi_n} = (1 - \lambda_n) b_{\mu_0} + \lambda_n b_\pi > 0$. In addition, V_{π_n} must be minimised at some point $z_{0,n} \in B(0, \sqrt{\frac{b_{\pi_n}}{a_{\pi_n}}})$, thus the Lipschitz assumptions imply

$$\|\nabla V_{\pi_n}(z)\|^2 \leq 2L_{\pi_n}^2 \left(\|z\|^2 + \frac{b_{\pi_n}}{a_{\pi_n}} \right). \quad (\text{B.13})$$

Lemma B.2. *Under Assumption 1 and 2, if $\gamma_n \geq 1$, we have for all $n \geq 1$*

$$\int [\mu_{n-1}(y) - \mu_{n-1/2}(y)] \log \frac{\pi(y)}{\mu_0(y)} dy \leq 2\gamma_n (A + B \mathbb{E}_{\mu_{n-1}}[\|Y\|^2]),$$

where

$$\begin{aligned} A &:= L_\pi + L_\pi \left(\frac{L_\pi b_\pi}{a_\pi} + \frac{L_{\mu_0} b_{\mu_0}}{a_{\mu_0}} \right) + \frac{L_{\mu_0} b_{\mu_0}}{a_{\mu_0}} + \left(\frac{L_\pi b_\pi}{a_\pi} \vee \frac{L_{\mu_0} b_{\mu_0}}{a_{\mu_0}} \right) \\ B &:= L_\pi (L_\pi + L_{\mu_0}) + L_{\mu_0} + (L_\pi \vee L_{\mu_0}). \end{aligned}$$

Proof. Using the definition of $\mu_{n-1/2}$ we have

$$\begin{aligned} \int [\mu_{n-1}(y) - \mu_{n-1/2}(y)] \log \frac{\pi(y)}{\mu_0(y)} dy &= \int [\mu_{n-1}(y) - \mu_{n-1} R_{\gamma_n}(y)] \log \frac{\pi(y)}{\mu_0(y)} dy \\ &= \int \mu_{n-1}(y) \left(\log \frac{\pi(y)}{\mu_0(y)} - R_{\gamma_n} \left(\log \frac{\pi}{\mu_0} \right) (y) \right) dy. \end{aligned}$$

Focusing on the integrand, we can write

$$\begin{aligned} \log \frac{\pi(y)}{\mu_0(y)} - R_{\gamma_n} \left(\log \frac{\pi}{\mu_0} \right) (y) &= [V_{\mu_0}(y) - V_\pi(y)] - (4\pi\gamma_n)^{-d/2} \int \exp \left(-\frac{1}{4\gamma_n} \|z - y - \gamma_n \nabla \log \pi_n(y)\|^2 \right) [V_{\mu_0}(z) - V_\pi(z)] dz \\ &= (4\pi\gamma_n)^{-d/2} \int \exp \left(-\frac{1}{4\gamma_n} \|z - y - \gamma_n \nabla \log \pi_n(y)\|^2 \right) [V_{\mu_0}(y) - V_\pi(y) - V_{\mu_0}(z) + V_\pi(z)] dz. \end{aligned}$$

We can then use Assumption 1 and 2 to obtain

$$V_{\mu_0}(y) - V_\pi(y) - V_{\mu_0}(z) + V_\pi(z) \leq \langle \nabla V_\pi(y) - \nabla V_{\mu_0}(y), z - y \rangle + (L_\pi - c_{\mu_0}) \|z - y\|^2,$$

for which the integral w.r.t. z can be computed analytically

$$\log \frac{\pi(y)}{\mu_0(y)} - R_{\gamma_n} \left(\log \frac{\pi}{\mu_0} \right) (y) \leq -\langle \nabla V_\pi(y) - \nabla V_{\mu_0}(y), \gamma_n \nabla V_{\pi_n}(y) \rangle + (L_\pi - c_{\mu_0}) (2\gamma_n + \gamma_n^2 \|\nabla V_{\pi_n}(y)\|^2).$$

Using the fact that $\nabla V_{\pi_n} = (1 - \lambda_n) \nabla V_{\mu_0} + \lambda_n \nabla V_\pi$ we then have

$$\begin{aligned} \log \frac{\pi(y)}{\mu_0(y)} - R_{\gamma_n} \left(\log \frac{\pi}{\mu_0} \right) (y) &\leq \|\nabla V_\pi(y)\|^2 ((L_\pi - c_{\mu_0}) \gamma_n^2 \lambda_n^2 - \gamma_n \lambda_n) + \|\nabla V_{\mu_0}(y)\|^2 ((L_\pi - c_{\mu_0}) \gamma_n^2 (1 - \lambda_n)^2 + \gamma_n (1 - \lambda_n)) \\ &\quad + 2\gamma_n (L_\pi - c_{\mu_0}) + (2\gamma_n \lambda_n - \gamma_n) \langle \nabla V_\pi(y), \nabla V_{\mu_0}(y) \rangle \\ &\leq \|\nabla V_\pi(y)\|^2 ((L_\pi - c_{\mu_0}) \gamma_n^2 \lambda_n^2 - \gamma_n \lambda_n) + \|\nabla V_{\mu_0}(y)\|^2 ((L_\pi - c_{\mu_0}) \gamma_n^2 (1 - \lambda_n)^2 + \gamma_n (1 - \lambda_n)) \\ &\quad + 2\gamma_n (L_\pi - c_{\mu_0}) + \gamma_n \lambda_n (\|\nabla V_\pi(y)\|^2 \vee \|\nabla V_{\mu_0}(y)\|^2), \end{aligned}$$

where we used the Cauchy-Schwarz inequality and the fact that $\lambda_n \leq 1$ for the last step. Using (B.3) and the equivalent result for μ_0 we further have

$$\begin{aligned} &\int \mu_{n-1}(y) \left(\log \frac{\pi(y)}{\mu_0(y)} - R_{\gamma_n} \left(\log \frac{\pi}{\mu_0} \right) (y) \right) dy \\ &\leq 2\gamma_n L_\pi + 2L_\pi \gamma_n^2 \left(\frac{L_\pi b_\pi}{a_\pi} + \frac{L_{\mu_0} b_{\mu_0}}{a_{\mu_0}} \right) + 2\gamma_n \frac{L_{\mu_0} b_{\mu_0}}{a_{\mu_0}} + 2\gamma_n \left(\frac{L_\pi b_\pi}{a_\pi} \vee \frac{L_{\mu_0} b_{\mu_0}}{a_{\mu_0}} \right) \\ &\quad + [2L_\pi \gamma_n^2 (L_\pi + L_{\mu_0}) + 2\gamma_n L_{\mu_0} + 2\gamma_n (L_\pi \vee L_{\mu_0})] \mathbb{E}_{\mu_{n-1}}[\|Y\|^2]. \end{aligned}$$

where we used again $\lambda_n \leq 1$ and removed the negative terms. Further assuming that $\gamma_n \leq 1$ we obtain

$$\begin{aligned} & \int \mu_{n-1}(y) \left(\log \frac{\pi(y)}{\mu_0(y)} - R_{\gamma_n} \left(\log \frac{\pi}{\mu_0} \right) (y) \right) dy \\ & \leq 2\gamma_n \left[L_\pi + L_\pi \left(\frac{L_\pi b_\pi}{a_\pi} + \frac{L_{\mu_0} b_{\mu_0}}{a_{\mu_0}} \right) + \frac{L_{\mu_0} b_{\mu_0}}{a_{\mu_0}} + \left(\frac{L_\pi b_\pi}{a_\pi} \vee \frac{L_{\mu_0} b_{\mu_0}}{a_{\mu_0}} \right) \right] \\ & \quad + 2\gamma_n [L_\pi (L_\pi + L_{\mu_0}) + L_{\mu_0} + (L_\pi \vee L_{\mu_0})] \mathbb{E}_{\mu_{n-1}}[\|Y\|^2], \end{aligned}$$

which gives the result. \square

Lemma B.3. *Under Assumption 1 and 2, if $\gamma_n \leq a_{\pi_n}/L_{\pi_n}^2$ we have*

$$\mathbb{E}_{\mu_n}[\|X\|^2] \leq \mathbb{E}_{\mu_0}[\|X\|^2] \left(\frac{d+b_\pi}{a_\pi} \right)^{\sum_{k=1}^n \delta_k} \prod_{k=1}^n Z_k^{-1} + 2(d+2(b_\pi \vee b_{\mu_0})) \sum_{k=1}^n \gamma_k \left(\frac{d+b_\pi}{a_\pi} \right)^{\sum_{i=k}^n \delta_k} \prod_{i=k}^n Z_i^{-1},$$

where $Z_k := \int \mu_{k-1/2}^{1-\delta_k}(x') \pi^{\delta_k}(x') dx'$ is the normalising constant of μ_k .

Proof. Using the definition (3.5) leads to

$$\mathbb{E}_{\mu_n}[\|X\|^2] = \int \|x\|^2 \frac{\mu_{n-1/2}^{1-\delta_n}(x) \pi^{\delta_n}(x)}{Z_n} dx,$$

where we defined $Z_n = \int \mu_{n-1/2}^{1-\delta_n}(x') \pi^{\delta_n}(x') dx'$. Applying Hölder inequality as in [CHH⁺23b, Appendix B] with $p = (1 - \delta_n)^{-1}$ and $q = \delta_n^{-1}$ gives

$$\begin{aligned} \int \|x\|^2 \frac{\mu_{n-1/2}^{1-\delta_n}(x) \pi^{\delta_n}(x)}{Z_n} dz &= \frac{1}{Z_n} \int (\|x\|^2 \mu_{n-1/2}(x))^{1-\delta_n} (\|x\|^2 \pi(x))^{\delta_n} dx \\ &\leq \frac{1}{Z_n} \left(\int \|x\|^2 \mu_{n-1/2}(x) dx \right)^{1-\delta_n} \left(\int \|x\|^2 \pi(x) dx \right)^{\delta_n} \\ &\leq \frac{\mathbb{E}_{\mu_{n-1/2}}[\|X\|^2]^{1-\delta_n}}{Z_n} \left(\frac{d+b_\pi}{a_\pi} \right)^{\delta_n}, \end{aligned}$$

where we used (B.2). It follows that

$$\mathbb{E}_{\mu_n}[\|X\|^2] \leq \frac{1}{Z_n} \left(\frac{d+b_\pi}{a_\pi} \right)^{\delta_n} \max(\mathbb{E}_{\mu_{n-1/2}}[\|X\|^2], 1) \leq \frac{1 + \mathbb{E}_{\mu_{n-1/2}}[\|X\|^2]}{Z_n} \left(\frac{d+b_\pi}{a_\pi} \right)^{\delta_n}. \quad (\text{B.14})$$

Using (3.7) and proceeding as in [CKSV25, Appendix B.3] we find

$$\begin{aligned} \mathbb{E}_{\mu_{n-1/2}}[\|X\|^2] &= \int \|x\|^2 \mu_{n-1/2}(x) dx \\ &= \int \|x\|^2 \int \mathcal{N}(x; z + \gamma_n \nabla \log \pi_n(z), 2\gamma_n \cdot \text{Id}) \mu_{n-1}(z) dz dx \\ &= \int (2d\gamma_n + \|z - \gamma_n \nabla V_{\pi_n}(z)\|^2) \mu_{n-1}(z) dz \\ &= 2d\gamma_n + \int \|z\|^2 \mu_{n-1}(z) dz + \int (\gamma_n^2 \|\nabla V_{\pi_n}(z)\|^2 - 2\gamma_n \langle z, \nabla V_{\pi_n}(z) \rangle) \mu_{n-1}(z) dz. \end{aligned}$$

Using (B.12) and (B.13) we obtain

$$\mathbb{E}_{\mu_{n-1/2}}[\|X\|^2] \leq (1 + 2\gamma_n^2 L_{\pi_n}^2 - 2\gamma_n a_{\pi_n}) \mathbb{E}_{\mu_{n-1}}[\|X\|^2] + 2d\gamma_n + 2\gamma_n^2 L_{\pi_n}^2 \frac{b_{\pi_n}}{a_{\pi_n}} + 2\gamma_n b_{\pi_n}.$$

If $\gamma_n \leq a_{\pi_n}/L_{\pi_n}^2$, and recalling that $b_{\pi_n} = \lambda_n b_\pi + (1 - \lambda_n) b_{\mu_0} \leq b_\pi \vee b_{\mu_0}$ we obtain

$$\begin{aligned} \mathbb{E}_{\mu_{n-1/2}}[\|X\|^2] &\leq \mathbb{E}_{\mu_{n-1}}[\|X\|^2] + 2\gamma_n (d + 2b_{\pi_n}) \\ &\leq \mathbb{E}_{\mu_{n-1}}[\|X\|^2] + 2\gamma_n (d + 2(b_\pi \vee b_{\mu_0})). \end{aligned} \quad (\text{B.15})$$

The result then follows by induction from (B.14) and (B.15). \square

B.3 Convergence of Sequential Monte Carlo Approximations

For any distribution η and any $\varphi \in \mathcal{B}_b(\mathbb{R}^d)$ we denote $\eta(\varphi) := \int \varphi(x)\eta(x)dx$, similarly for all empirical distributions $\eta^N := N^{-1} \sum_{i=1}^N \delta_{X^i}$ we denote the corresponding average by $\eta^N(\varphi) := N^{-1} \sum_{i=1}^N \varphi(X^i)$.

At time n , we denote the target distribution (also known as updated distribution) as $\hat{\eta}_n$, convolving the proposal kernel M_n with $\hat{\eta}_{n-1}$ we obtain the mutated distribution η_n in (corresponding to $\mu_{n-1/2}$ for Tempered WFR and WFR. We observe that the target distribution can be obtained from the mutated one as

$$\hat{\eta}_n(\varphi) = \frac{\eta_n(w_n \varphi)}{\eta_n(w_n)} = \Psi_{w_n}(\eta_n).$$

The particle approximations to the quantities above obtained via SMC are as follows: the particle approximation to η_n is denoted by $\eta_n^N = N^{-1} \sum_{i=1}^N \delta_{X_n^i}$, $\Psi_{w_n^N}(\eta_n^N) = \sum_{i=1}^N W_n^i \delta_{X_n^i}$ and $\hat{\eta}_n^N = N^{-1} \sum_{i=1}^N \delta_{\tilde{X}_n^i}$ both approximate $\Psi_{w_n}(\eta_n) = \hat{\eta}_n$.

We consider the case in which the true weights w_n are intractable and need to be approximated; in particular we focus on approximations of the form

$$w_n^N(x) := \frac{\eta_n(x)}{\int M_n(z, x) \Psi_{w_{n-1}^N}(\eta_{n-1}^N)(z) dz} = \frac{\left(\int M_n(z, x) \Psi_{w_{n-1}^N}(\eta_{n-1}^N)(z) dz \right)^{1-\delta} \pi^\delta(x)}{\int M_n(z, x) \Psi_{w_{n-1}^N}(\eta_{n-1}^N)(z) dz}, \quad (\text{B.16})$$

which corresponds to that of the algorithms described in Section 4.3. Other weight approximations of this type have been considered in [CJ23].

Proof of 4.1. The proof follows an inductive argument. For the case $n = 0$ we use the fact that $w_0^N \equiv w_0$ and the WLLN for self normalized importance sampling (e.g. [CMR05, Theorem 9.1.8]) to show $\Psi_{w_0^N}(\eta_0^N)(\varphi) \xrightarrow{P} \Psi_{w_0}(\eta_0)(\varphi)$. Lemma B.5–B.9 below show that if the result holds at time $n - 1$ then it also holds at time n . We then conclude the proof using induction. \square

B.3.1 Auxiliary results for the proof of Proposition 4.1

As a preliminary we reproduce part of [dM04, Lemma 7.3.3], a Marcinkiewicz-Zygmund-type inequality of which we will make extensive use.

Lemma B.4 (Del Moral, 2004). *Given a sequence of probability measures $(\mu_i)_{i \geq 1}$ on a given measurable space (E, \mathcal{E}) and a collection of independent random variables, one distributed according to each of those measures, $(X_i)_{i \geq 1}$, where $\forall i, X_i \sim \mu_i$, together with any sequence of measurable functions $(h_i)_{i \geq 1}$ such that $\mu_i(h_i) = 0$ for all $i \geq 1$, we define for any $N \in \mathbb{N}$,*

$$m_N(X)(h) = \frac{1}{N} \sum_{i=1}^N h_i(X_i) \quad \text{and} \quad \sigma_N^2(h) = \frac{1}{N} \sum_{i=1}^N (\sup(h_i) - \inf(h_i))^2.$$

If the h_i have finite oscillations (i.e., $\sup(h_i) - \inf(h_i) < \infty \forall i \geq 1$) then we have:

$$\sqrt{N} \mathbb{E} [|m_N(X)(h)|^p]^{1/p} \leq b(p)^{1/p} \sigma_N(h),$$

with, for any pair of integers q, p such that $q \geq p \geq 1$, denoting $(q)_p = q! / (q - p)!$:

$$b(2q) = (2q)_q 2^{-q} \quad \text{and} \quad b(2q - 1) = \frac{(2q - 1)_q}{\sqrt{q - \frac{1}{2}}} 2^{-(q - \frac{1}{2})}. \quad (\text{B.17})$$

We collect here four auxiliary results for the proof of the WLLN in Proposition 4.1. In particular, Lemma B.5, B.8, and B.9 can be found in [CMR05, Section 9.3] while Proposition B.6 is adapted from [CJ23].

Lemma B.5 (Mutation). *Assume that, for any $\varphi \in \mathcal{B}_b(\mathbb{R}^d)$, $\hat{\eta}_{n-1}^N(\varphi) \xrightarrow{P} \hat{\eta}_{n-1}(\varphi)$, then, after the mutation step, $\eta_n^N(\varphi) \xrightarrow{P} \eta_n(\varphi)$ for any $\varphi \in \mathcal{B}_b(\mathbb{R}^d)$.*

Proof. Let \mathcal{G}_{n-1}^N denote the σ -field generated by the particle system up to (and including) time $n-1$ before the mutation step at time n , $\mathcal{G}_{n-1}^N = \sigma(\tilde{X}_p^i : i \in \{1, \dots, N\}) \vee \mathcal{F}_{n-1}^N$ and consider the sequence of functions $\Delta_n^i : E \mapsto \mathbb{R}$ for $i = 1, \dots, N$, $\Delta_n^i(x) := \varphi(x) - \mathbb{E}[\varphi(X_n^i) | \mathcal{G}_{n-1}^N] = \varphi(x) - M_n \varphi(\tilde{X}_{n-1}^i)$. Conditionally on \mathcal{G}_{n-1}^N , $\Delta_n^i(X_n^i)$, $i = 1, \dots, N$ are independent and have expectation equal to 0, moreover

$$\eta_n^N(\varphi) - \hat{\eta}_{n-1}^N M_n(\varphi) = \frac{1}{N} \sum_{i=1}^N [\varphi(X_n^i) - M_n \varphi(\tilde{X}_{n-1}^i)] = \frac{1}{N} \sum_{i=1}^N \Delta_n^i(X_n^i).$$

Conditioning on \mathcal{G}_{n-1}^N and applying Lemma B.4 we have, for all $p \geq 1$,

$$\begin{aligned} \sqrt{N} \mathbb{E} [|\eta_n^N(\varphi) - \hat{\eta}_{n-1}^N M_n(\varphi)|^p | \mathcal{G}_{n-1}^N]^{1/p} &\leq b(p)^{1/p} \frac{1}{\sqrt{N}} \left(\sum_{i=1}^N (\sup(\Delta_n^i) - \inf(\Delta_n^i))^2 \right)^{1/2} \\ &\leq b(p)^{1/p} \frac{1}{\sqrt{N}} \left(\sum_{i=1}^N 4 (\sup |\Delta_n^i|)^2 \right)^{1/2} \\ &\leq b(p)^{1/p} \frac{1}{\sqrt{N}} \left(\sum_{i=1}^N 16 \|\varphi\|_\infty^2 \right)^{1/2} \\ &\leq 4b(p)^{1/p} \|\varphi\|_\infty \end{aligned} \quad (\text{B.18})$$

with $b(p)$ as in (B.17).

Using (B.18) and Markov's inequality, it follows that $\eta_n^N(\varphi) - \hat{\eta}_{n-1}^N M_n(\varphi) \xrightarrow{P} 0$. We can use the hypothesis to get $\hat{\eta}_{n-1}^N M_n(\varphi) \xrightarrow{P} \hat{\eta}_{n-1} M_n(\varphi)$. Combining the two results above and using Slutsky's lemma we obtain $\eta_n^N(\varphi) \xrightarrow{P} \eta_n(\varphi)$. \square

Proposition B.6. *Let \mathcal{F}_{n-1}^N denote the σ -field generated by the weighted samples up to (and including) time $n-1$. We have $\mathbb{E}[\eta_n^N(w_n^N \varphi) | \mathcal{F}_{n-1}^N] = \int \varphi(x_n) \left(M_n \Psi_{w_{n-1}^N}(\eta_{n-1}^N)(x_n) \right)^{1-\delta} \pi^\delta(x_n) dx_n$, for all $n \geq 1$ and all $\varphi \in \mathcal{B}_b(\mathbb{R}^d)$. In addition, $\eta_n(w_n \varphi) = \int \varphi(x_n) (\hat{\eta}_{n-1} M_n(x_n))^{1-\delta} \pi^\delta(x_n) dx_n$.*

Proof. Consider the conditional expectation

$$\begin{aligned} \mathbb{E}[\eta_n^N(w_n^N \varphi) | \mathcal{F}_{n-1}^N] &= \frac{1}{N} \sum_{i=1}^N \mathbb{E}[w_n^N(X_n^i) \varphi(X_n^i) | \mathcal{F}_{n-1}^N] \\ &= \frac{1}{N} \sum_{i=1}^N \mathbb{E}[\mathbb{E}[w_n^N(X_n^i) \varphi(X_n^i) | \mathcal{G}_{n-1}^N] | \mathcal{F}_{n-1}^N] \\ &= \frac{1}{N} \sum_{i=1}^N \mathbb{E} \left[\int M_n(\tilde{X}_{n-1}^i, dx_n) w_n^N(x_n) \varphi(x_n) | \mathcal{F}_{n-1}^N \right] \\ &= \sum_{j=1}^N \frac{w_{n-1}^N(X_{n-1}^j)}{\sum_{k=1}^N w_{n-1}^N(X_{n-1}^k)} \int M_n(X_{n-1}^j, x_n) w_n^N(x_n) \varphi(x_n) dx_n, \end{aligned}$$

where the third equality follows from the fact that $X_n^i | \mathcal{G}_{n-1}^N \sim M_n(\tilde{X}_{n-1}^i, \cdot)$ for each $i = 1, \dots, N$ and the fourth from the fact that $\{X_{n-1}^j\}_{j=1}^N$ and w_{n-1}^N are \mathcal{F}_{n-1}^N -measurable and conditionally each \tilde{X}_{n-1}^i is drawn independently from the categorical distribution with probabilities given by the weights. Plugging the

definition of w_n^N in (B.16) into the above we obtain

$$\begin{aligned}
& \mathbb{E} [\eta_n^N(w_n^N \varphi) \mid \mathcal{F}_{n-1}^N] \\
&= \int \int M_n(x_{n-1}, x_n) \varphi(x_n) \Psi_{w_{n-1}^N}(\eta_{n-1}^N)(x_{n-1}) \frac{\left(\int M_n(z, x_n) \Psi_{w_{n-1}^N}(\eta_{n-1}^N)(z) dz \right)^{1-\delta} \pi^\delta(x_n)}{\int M_n(z, x_n) \Psi_{w_{n-1}^N}(\eta_{n-1}^N)(z) dz} dx_n dx_{n-1} \\
&= \int \varphi(x_n) \left(\int M_n(z, x_n) \Psi_{w_{n-1}^N}(\eta_{n-1}^N)(z) dz \right)^{1-\delta} \pi^\delta(x_n) dx_n \\
&= \int \varphi(x_n) \left(M_n \Psi_{w_{n-1}^N}(\eta_{n-1}^N)(x_n) \right)^{1-\delta} \pi^\delta(x_n) dx_n.
\end{aligned}$$

We have that, for all $n \geq 1$ and all $\varphi \in \mathcal{B}_b(\mathbb{R}^d)$,

$$\begin{aligned}
\eta_n(w_n \varphi) &= \int \varphi(x_n) G_n(x_n) \eta_n(x_n) dx_n \\
&= \int \int M_n(x_{n-1}, x_n) \varphi(x_n) \frac{(\hat{\eta}_{n-1} M_n(x_n))^{1-\delta} \pi^\delta(x_n)}{\hat{\eta}_{n-1} M_n(x_n)} \hat{\eta}_{n-1}(x_{n-1}) dx_n dx_{n-1} \\
&= \int \varphi(x_n) (\hat{\eta}_{n-1} M_n(x_n))^{1-\delta} \pi^\delta(x_n) dx_n.
\end{aligned}$$

□

Lemma B.7 (Weight Comparison). *Assume that for any $\varphi \in \mathcal{B}_b(\mathbb{R}^d)$, $\Psi_{w_{n-1}^N}(\eta_{n-1}^N)(\varphi) \xrightarrow{p} \Psi_{w_{n-1}}(\eta_{n-1})(\varphi)$, then $\eta_n^N(w_n^N \varphi) \xrightarrow{p} \eta_n(w_n \varphi)$, for any $\varphi \in \mathcal{B}_b(\mathbb{R}^d)$.*

Proof. Consider the decomposition

$$\eta_n^N(w_n^N \varphi) - \eta_n(w_n \varphi) = \eta_n^N(w_n^N \varphi) - \mathbb{E} [\eta_n^N(w_n^N \varphi) \mid \mathcal{F}_{n-1}^N] + \mathbb{E} [\eta_n^N(w_n^N \varphi) \mid \mathcal{F}_{n-1}^N] - \eta_n(w_n \varphi).$$

For the first term, consider the sequence of functions $\Delta_n^i : E \mapsto \mathbb{R}$, $\Delta_n^i(x) := w_n^N(x) \varphi(x) - \mathbb{E} [w_n^N(X_n^i) \varphi(X_n^i) \mid \mathcal{F}_{n-1}^N]$, for $i = 1, \dots, N$. Conditionally on \mathcal{F}_{n-1}^N , $\Delta_n^i(X_n^i)$ $i = 1, \dots, N$ are independent and have expectation equal to 0, moreover

$$\eta_n^N(w_n^N \varphi) - \mathbb{E} [\eta_n^N(w_n^N \varphi) \mid \mathcal{F}_{n-1}^N] = \frac{1}{N} \sum_{i=1}^N \Delta_n^i(X_n^i).$$

Using Lemma B.4, we have almost surely

$$\sqrt{N} \mathbb{E} [\eta_n^N(w_n^N \varphi) - \mathbb{E} [\eta_n^N(w_n^N \varphi) \mid \mathcal{F}_{n-1}^N] \mid \mathcal{F}_{n-1}^N]^{1/p} \leq 4b(p)^{1/p} \|w_n^N\|_\infty \|\varphi\|_\infty,$$

where $b(p)$ is given in (B.17). Hence, by Markov's inequality, $\eta_n^N(w_n^N \varphi) - \mathbb{E} [\eta_n^N(w_n^N \varphi) \mid \mathcal{F}_{n-1}^N] \xrightarrow{p} 0$.

Using Proposition B.6, the dominated convergence theorem and the hypothesis we have

$$\mathbb{E} [\eta_n^N(w_n^N \varphi) \mid \mathcal{F}_{n-1}^N] \xrightarrow{p} \eta_n(w_n \varphi),$$

from which the result follows. □

Lemma B.8 (Approximate reweighting). *Assume that, for any $\varphi \in \mathcal{B}_b(\mathbb{R}^d)$, $\eta_n^N(w_n^N \varphi) \xrightarrow{p} \eta_n(w_n \varphi)$, then $\Psi_{w_n^N}(\eta_n^N)(\varphi) \xrightarrow{p} \Psi_{w_n}(\eta_n)(\varphi)$ for any $\varphi \in \mathcal{B}_b(\mathbb{R}^d)$.*

Proof. Take the definition of Ψ_{w_n} and $\Psi_{w_n^N}$, $\Psi_{w_n^N}(\eta_n^N)(\varphi) - \Psi_{w_n}(\eta_n)(\varphi) = \frac{\eta_n^N(w_n^N \varphi)}{\eta_n^N(w_n^N)} - \frac{\eta_n(w_n \varphi)}{\eta_n(w_n)}$. A simple application of the continuous mapping theorem to the hypothesis gives $\frac{\eta_n^N(w_n^N \varphi)}{\eta_n^N(w_n^N)} \xrightarrow{p} \frac{\eta_n(w_n \varphi)}{\eta_n(w_n)}$, and the result follows. □

Lemma B.9 (Multinomial resampling). *Assume that, for any $\varphi \in \mathcal{B}_b(\mathbb{R}^d)$, $\Psi_{w_n^N}(\eta_n^N)(\varphi) \xrightarrow{P} \hat{\eta}_n(\varphi)$, then after the resampling step performed through multinomial resampling $\hat{\eta}_n^N(\varphi) \xrightarrow{P} \hat{\eta}_n(\varphi)$ for any $\varphi \in \mathcal{B}_b(\mathbb{R}^d)$.*

Proof. Consider the decomposition

$$\hat{\eta}_n^N(\varphi) - \hat{\eta}_n(\varphi) = \hat{\eta}_n^N(\varphi) - \Psi_{w_n^N}(\eta_n^N)(\varphi) + \Psi_{w_n^N}(\eta_n^N)(\varphi) - \hat{\eta}_n(\varphi).$$

Denote by \mathcal{F}_n^N the σ -field generated by the weighted samples up to (and including) time n , $\mathcal{F}_n^N := \sigma(X_n^i : i \in \{1, \dots, N\}) \vee \mathcal{G}_{n-1}^N$ and consider the sequence of functions $\Delta_n^i : \mathbb{R}^d \mapsto \mathbb{R}$, $\Delta_n^i(x) := \varphi(x) - \mathbb{E}[\varphi(\tilde{X}_n^i) | \mathcal{F}_n^N]$, for $i = 1, \dots, N$. Conditionally on \mathcal{F}_n^N , $\Delta_n^i(\tilde{X}_n^i)$ $i = 1, \dots, N$ are independent and have expectation equal to 0, moreover

$$\hat{\eta}_n^N(\varphi) - \Psi_{w_n^N}(\eta_n^N)(\varphi) = \frac{1}{N} \sum_{i=1}^N \left(\varphi(\tilde{X}_n^i) - \mathbb{E}[\varphi(\tilde{X}_n^i) | \mathcal{F}_n^N] \right) = \frac{1}{N} \sum_{i=1}^N \Delta_n^i(\tilde{X}_n^i).$$

Using Lemma B.4, we find

$$\sqrt{N} \mathbb{E} \left[|\hat{\eta}_n^N(\varphi) - \Psi_{w_n^N}(\eta_n^N)(\varphi)|^p \mid \mathcal{F}_n^N \right]^{1/p} \leq 4b(p)^{1/p} \|\varphi\|_\infty, \quad (\text{B.19})$$

where $b(p)$ is as in (B.17). Using (B.19) and Markov's inequality, we have that $\hat{\eta}_n^N(\varphi) - \Psi_{w_n^N}(\eta_n^N)(\varphi) \xrightarrow{P} 0$.

Since $\hat{\eta}_n(\varphi) \equiv \Psi_{w_n}(\eta_n)(\varphi)$, this result combined with the hypothesis yields $\hat{\eta}_n^N(\varphi) \xrightarrow{P} \hat{\eta}_n(\varphi)$. \square

C Analytic solutions: Multivariate Gaussian case

This section focuses on comparing the evolution of the PDEs introduced in this section for the special case of transporting a Gaussian $\mu_0(x) = \mathcal{N}(x; m_0, C_0)$ to target Gaussian $\pi(x) = \mathcal{N}(x; m_\pi, C_\pi)$. In this case, we can obtain nice expressions for the moments along the flow described by each PDE.

In particular, observing that both the tempered W flow and the tempered FR flow preserve gaussianity, we have that $\mu_t(x) = \mathcal{N}(x; m_t, C_t)$ for each time $t \geq 0$.

We detail here the results needed to obtain the ODEs describing the tempered and standard PDEs for the special case of transporting a Gaussian $\mu_0(x) = \mathcal{N}(x; m_0, C_0)$ to target Gaussian $\pi(x) = \mathcal{N}(x; m_\pi, C_\pi)$.

Wasserstein Flow (Langevin) The PDE in this case is the Fokker-Planck equation for the overdamped Langevin SDE

$$\begin{aligned} dX_t &= -\nabla V_\pi(X_t) dt + \sqrt{2} dB_t \\ &= -C_\pi^{-1}(X_t - m_\pi) dt + \sqrt{2} dB_t. \end{aligned}$$

Since the potential takes the form $V_\pi(x) = \frac{1}{2}(x - m_\pi)^\top C_\pi^{-1}(x - m_\pi)$, the moment equations are standard as this essentially boils down to an Ornstein-Uhlenbeck process. They are given by

$$\begin{aligned} \dot{m}_t &= -C_\pi^{-1}(m_t - m_\pi) \\ \dot{C}_t &= -C_\pi^{-1}C_t - C_t C_\pi^{-1} + 2I \end{aligned}$$

and the explicit solution can be found as

$$\begin{aligned} m_t &= e^{-tC_\pi^{-1}} m_0 + (I - e^{-tC_\pi^{-1}}) m_\pi \\ C_t &= e^{-tC_\pi^{-1}} \left(2 \int_0^t e^{sC_\pi^{-1}} (e^{sC_\pi^{-1}})^\top ds + C_0 \right) (e^{-tC_\pi^{-1}})^\top. \end{aligned}$$

In the 1D case, we can easily evaluate the expression for C_t as

$$C_t = e^{-2tC_\pi^{-1}} [C_0 + C_\pi (e^{2tC_\pi^{-1}} - 1)].$$

Fisher–Rao flow In the Gaussian case, the ODEs for the mean and covariance respectively are given by

$$\begin{aligned}\dot{m}_t &= -C_t C_\pi^{-1} (m_t - m_\pi) \\ \dot{C}_t &= -C_t C_\pi^{-1} C_t + C_t.\end{aligned}$$

The explicit solutions in this case are known (see e.g. [CHH⁺23a, Proposition 4.11]),

$$\begin{aligned}m_t &= m_\pi + e^{-t} \left((1 - e^{-t}) C_\pi^{-1} + e^{-t} C_0^{-1} \right)^{-1} C_0^{-1} (m_0 - m_\pi) \\ &= m_\pi + e^{-t} C_t C_0^{-1} (m_0 - m_\pi) \\ C_t^{-1} &= C_\pi^{-1} + e^{-t} (C_0^{-1} - C_\pi^{-1}).\end{aligned}$$

Unit time Fisher–Rao flow The evolution of m_t, C_t along the unit time FR flow (2.4) is given by

$$\begin{aligned}m_t &= C_t \left[(1 - t) C_0^{-1} m_0 + t C_\pi^{-1} m_\pi \right] \\ C_t &= \left[(1 - t) C_0^{-1} + t C_\pi^{-1} \right]^{-1}\end{aligned}$$

Clearly at $t = 1, m_t = m_\pi, C_t = C_\pi$. The unit time FR and the infinite time FR follow the same path but over different time-scales which can be connected using the time scaling in Lemma A.2.

Wasserstein–Fisher–Rao flow The mean and covariance equations in the Gaussian case for the Wasserstein–Fisher–Rao flow can be obtained using the results for the pure Wasserstein and pure Fisher–Rao flows as shown in [LMTZ25, Proposition 2.2],

$$\begin{aligned}\dot{m}_t &= -(C_t + I) C_\pi^{-1} (m_t - m_\pi) \\ \dot{C}_t &= -C_t C_\pi^{-1} C_t + C_t - C_\pi^{-1} C_t - C_t C_\pi^{-1} + 2I\end{aligned}$$

The explicit solution in the 1D case is given by

$$\begin{aligned}C_t &= C_\pi + \frac{1}{\left(\frac{1}{C_0 - C_\pi} + \frac{1}{C_\pi + 2} \right) e^{\left(1 + \frac{2}{C_\pi}\right)t} - \frac{1}{C_\pi + 2}} \\ m_t &= m_\pi + (m_0 - m_\pi) \exp\left(\frac{t}{C_\pi}\right) \frac{C_t - C_\pi}{C_0 - C_\pi},\end{aligned}$$

showing that C_t must approach C_π faster than $\exp(t/C_\pi)$ grows, which is guaranteed by the factor 2 in the expression for C_t . Explicit solution of the covariance evolution under the WFR flow are give in [LMTZ25, Remark 2.3].

Tempered Wasserstein flow (Tempered Langevin; [CKSV25]) Recall the diffusion process characterising Tempered Langevin is given by

$$dX_t = -\left[(1 - \lambda_t) \nabla_x V_{\mu_0} + \lambda_t \nabla_x V_\pi \right] dt + \sqrt{2} dB_t$$

where $\lambda_t : \mathbb{R}_+ \rightarrow [0, 1)$ is a non-decreasing function of t . The corresponding evolution PDE given by

$$\partial_t \mu_t(x) = \nabla \cdot \left(\mu_t(x) \nabla \log \left(\frac{\mu_t(x)}{\pi_t(x)} \right) \right) = \nabla \cdot \left(\mu_t(x) \nabla \log \left(\frac{\mu_t(x)}{\pi(x)} \right)^{\lambda_t} \right) + \nabla \cdot \left(\mu_t(x) \nabla \log \left(\frac{\mu_t(x)}{\mu_0(x)} \right)^{1 - \lambda_t} \right)$$

where $\pi_t \propto \pi^{\lambda_t} \mu_0^{1 - \lambda_t}$. The second equality shows that it can be seen as a sum of two Wasserstein parts with temperatures λ_t and $1 - \lambda_t$.

Note that π_t is a product of 2 Gaussian densities $\mathcal{N}\left(m_\pi, \frac{C_\pi}{\lambda_t}\right)$ and $\mathcal{N}\left(m_0, \frac{C_0}{1 - \lambda_t}\right)$ therefore $\pi_t \propto \mathcal{N}(a_t, P_t)$ where

$$\begin{aligned}a_t &= \left(m_0 \frac{C_\pi}{\lambda_t} + m_\pi \frac{C_0}{1 - \lambda_t} \right) \left(\frac{C_0}{1 - \lambda_t} + \frac{C_\pi}{\lambda_t} \right)^{-1} \\ P_t &= C_\pi (\lambda_t C_0 + (1 - \lambda_t) C_\pi)^{-1} C_0\end{aligned}$$

and the intermediate densities are still Gaussian. Then we have the same structure for the moment ODEs as for infinite time Wasserstein gradient flow, except with m_π, C_π replaced by a_t, P_t respectively,

$$\begin{aligned}\dot{m}_t &= -\left(C_\pi(\lambda_t C_0 + (1 - \lambda_t)C_\pi)^{-1}C_0\right)^{-1} \left(m_t - \left(m_0 \frac{C_\pi}{\lambda_t} + m_\pi \frac{C_0}{1 - \lambda_t}\right) \left(\frac{C_0}{1 - \lambda_t} + \frac{C_\pi}{\lambda_t}\right)^{-1}\right) \\ &= -(\lambda_t C_\pi^{-1} + (1 - \lambda_t)C_0^{-1}) \left(m_t - ((1 - \lambda_t)m_0 C_\pi + \lambda_t m_\pi C_0) (\lambda_t C_0 + (1 - \lambda_t)C_\pi)^{-1}\right) \\ \dot{C}_t &= -\left(C_\pi(\lambda_t C_0 + (1 - \lambda_t)C_\pi)^{-1}C_0\right)^{-1} C_t - C_t \left(C_\pi(\lambda_t C_0 + (1 - \lambda_t)C_\pi)^{-1}C_0\right)^{-1} + 2I \\ &= -(\lambda_t C_\pi^{-1} + (1 - \lambda_t)C_0^{-1})C_t - C_t(\lambda_t C_\pi^{-1} + (1 - \lambda_t)C_0^{-1}) + 2I.\end{aligned}$$

In the 1D case, the explicit solution is given by

$$\begin{aligned}m_t &= m_0 e^{-\int_0^t (1 - \lambda_s) ds C_0^{-1} - \int_0^t \lambda_s ds C_\pi^{-1}} \\ &\quad + e^{-\int_0^t (1 - \lambda_s) ds C_0^{-1} - \int_0^t \lambda_s ds C_\pi^{-1}} \int_0^t [(1 - \lambda_u)C_0^{-1}m_0 + \lambda_u C_\pi^{-1}m_\pi] e^{\int_0^u (1 - \lambda_s) ds C_0^{-1} + \int_0^u \lambda_s ds C_\pi^{-1}} du \\ C_t &= C_0 e^{-2\int_0^t (1 - \lambda_s) ds C_0^{-1} - 2\int_0^t \lambda_s ds C_\pi^{-1}} \\ &\quad + 2e^{-2\int_0^t (1 - \lambda_s) ds C_0^{-1} - 2\int_0^t \lambda_s ds C_\pi^{-1}} \int_0^t e^{2\int_0^u (1 - \lambda_s) ds C_0^{-1} + 2\int_0^u \lambda_s ds C_\pi^{-1}} du.\end{aligned}$$

Tempered Fisher–Rao flow Recalling that $\pi_t \propto \mathcal{N}(a_t, P_t)$ with a_t, P_t as before and observing that tempered FR PDE can be written as

$$\begin{aligned}\partial_t \mu_t &= \mu_t(x) \left(\log \left(\frac{\pi_t(x)}{\mu_t(x)} \right) - \mathbb{E}_{\mu_t} \left[\log \left(\frac{\pi_t}{\mu_t} \right) \right] \right) \\ &= \mu_t(x) \left(\log \left(\frac{\pi(x)}{\mu_t(x)} \right)^{\lambda_t} - \mathbb{E}_{\mu_t} \left[\log \left(\frac{\pi}{\mu_t} \right)^{\lambda_t} \right] \right) + \mu_t(x) \left(\log \left(\frac{\mu_0(x)}{\mu_t(x)} \right)^{1 - \lambda_t} - \mathbb{E}_{\mu_t} \left[\log \left(\frac{\mu_0}{\mu_t} \right)^{1 - \lambda_t} \right] \right),\end{aligned}$$

we see that the tempered FR PDE is the sum of two Fisher–Rao paths with temperatures λ_t and $1 - \lambda_t$.

The ODEs describing the evolution of the moments of μ_t are obtained from those for the standard FR flow replacing m_π, C_π with a_t, P_t

$$\begin{aligned}\dot{m}_t &= -C_t(\lambda_t C_\pi^{-1} + (1 - \lambda_t)C_0^{-1})(m_t - m_\pi) \\ \dot{C}_t &= -C_t(\lambda_t C_\pi^{-1} + (1 - \lambda_t)C_0^{-1})C_t + C_t.\end{aligned}$$

D Algorithms and Additional Experimental Results

D.1 Birth Death Langevin Algorithms

The birth-death Langevin algorithm of [LLN19] is given in Algorithm 3. [LSW23] replace the average rate in Algorithm 3 is replaced by $\bar{\beta}_i = \beta_i - N^{-1} \sum_{j=1}^N \beta_j + \sum_{j=1}^N \frac{K(X_n^i - X_n^j)}{\sum_{i=1}^N K(X_n^j - X_n^i)} - 1$.

D.2 Additional results for Gaussian Mixture

We consider the decay of the MMD with Gaussian kernel along the W and WFR flows for the Gaussian mixture target

$$\mu_0(x) = \mathcal{N}(x; 0, 1), \quad \pi(x) = \frac{1}{2}\mathcal{N}(x; 0, 1) + \frac{1}{2}\mathcal{N}(x; m, 1).$$

This target satisfies a log-Sobolev inequality [Sch19] with $C_{\text{LSI}} = (1 + (e^{m^2} + 1)/2)$. The initial distribution is $\mu_0(x) = \mathcal{N}(x; 0, 1)$, WFR is run with $N = 500$ particles for 200 iterations and $\gamma = 0.1$. The results for ULA show the MMD of $N = 500$ independent chains ran for 2000 iterations with $\gamma = 0.1$.

Figure 4.1 shows the convergence of W and WFR against wallclock time for different values of m .

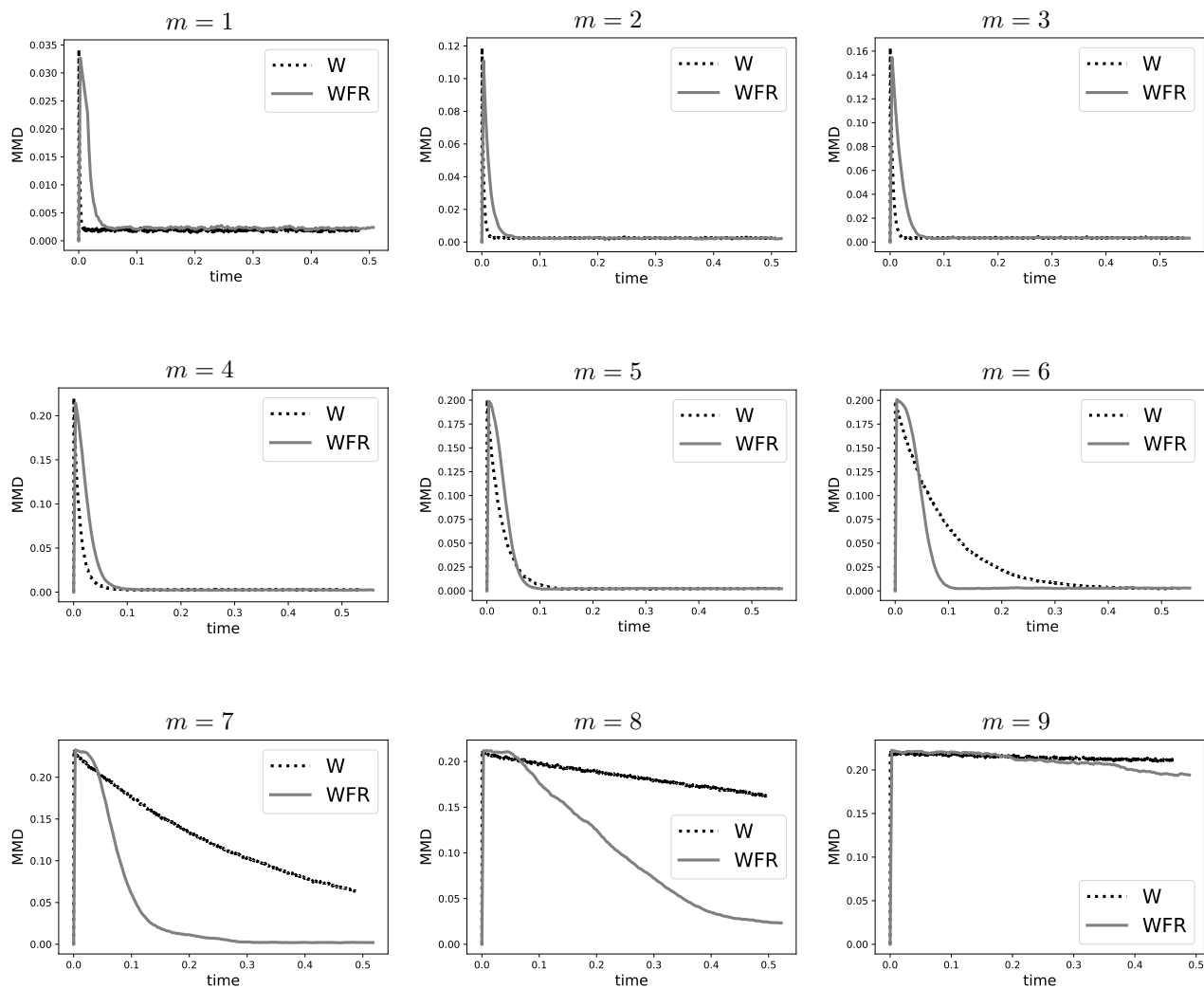


Figure 4.1: Convergence of approximations to π given W and WFR PDE flow with target the Gaussian mixture (5.1). Convergence is measured through the MMD with standard Gaussian kernel and is averaged over 50 replications. We show values of m from 1 to 9.

Algorithm 3 Birth-death accelerate Langevin algorithm (BDL; [LLN19])

Inputs: Discretisation steps $(\gamma_n)_{n=1,\dots,T}$, kernel function K , initial proposal μ_0 .

Initialize: sample $X_0^i \sim \mu_0$ for $i = 1, \dots, N$.

for $n = 1, \dots, T$ **do**

Langevin step: $X_n^i = X_{n-1}^i + \gamma_n \nabla \log \pi(X_{n-1}^i) + \sqrt{2\gamma_n} \xi_i$ where $\xi_i \sim \mathcal{N}(0, 1)$ for $i = 1, \dots, N$.

Birth-death step: compute the rate

$$\beta_i = \log \left(N^{-1} \sum_{j=1}^N K(X_n^i - X_n^j) \right) - \log \pi(X_n^i)$$

for $i = 1, \dots, N$.

Birth-death step: set $\bar{\beta}_i = \beta_i - N^{-1} \sum_{j=1}^N \beta_j$. If $\bar{\beta}_i > 0$ kill X_n^i with probability $1 - \exp(-\bar{\beta}_i \gamma_n)$, otherwise duplicate X_n^i w.p. $1 - \exp(\bar{\beta}_i \gamma_n)$.

Resampling: Let N_1 denote the current number of particles.

if $N_1 > N$ **then**

Kill $N_1 - N$ randomly selected particles.

else

Duplicate $N - N_1$ randomly selected particles.

end if

end for

Output: $\{X_n^i\}_{i=1}^N$.
